Stock assessment of Falkland calamari *Doryteuthis gahi* in the 2nd season 2025

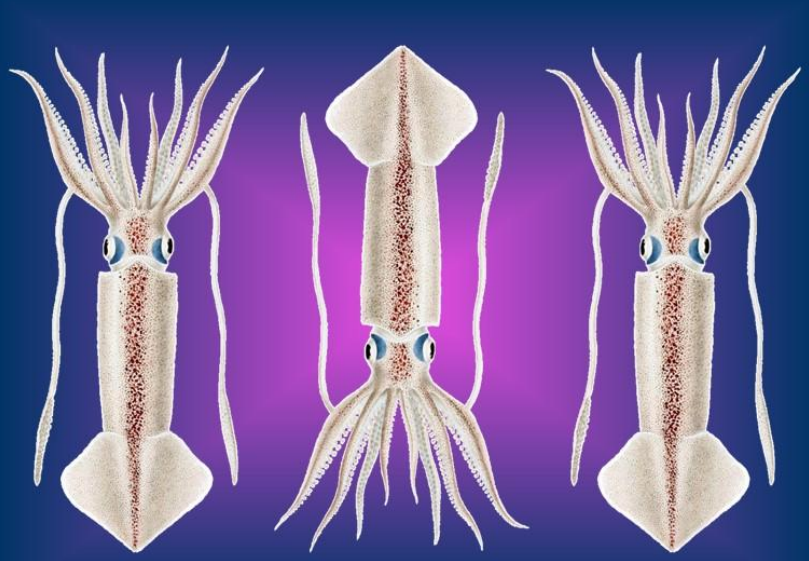

Skeljo F · Winter A

Fisheries Department
Directorate of Natural Resources
Falkland Islands Government
Stanley, Falkland Islands

October 2025

2025 – S2 – LOL

Participating Scientific Staff

Frane Skeljo (PhD, Senior Stock Assessment Scientist)
Andreas Winter (PhD, Head of Science)

Acknowledgements

We thank all the observers and researchers who have contributed to the data used in this stock assessment report.

© Crown Copyright 2025

For citation purposes, this publication should be referenced as follows:

Skeljo F, Winter A. 2025. Stock assessment of Falkland calamari (*Doryteuthis gahi*) in the 2nd season 2025. Technical Document, Falkland Islands Fisheries Department. 35 p.

Distribution: Public Domain

Reviewed and approved by:

James Wilson — Date: October 2025
Director of Natural Resources

Index

Summary

1) The 2nd season 2025 *Doryteuthis gahi* fishery (X licence) started on July 27th and finished on September 19th following a closure order. Two bad weather days were claimed by the fleet on August 13th and 14th, with no vessels fishing. The season lasted 55 days: 53 fishing and two non-fishing days.
2) 18,454 tonnes of *D. gahi* were reported caught under the X licence, giving an average CPUE of 21.8 tonnes per vessel-day. Both total catch and average CPUE were around 20% lower than the long-term average for the 2nd season.
3) The same two immigration peaks were inferred in both the North and South sub-areas: July 27th (the start of the season) and August 6th.
4) 22,002 tonnes of *D. gahi* (95% CI: 10,981 – 30,770 tonnes) were estimated to have immigrated into the Loligo Box on August 6th; 6,636 tonnes in the north and 15,366 tonnes in the south sub-area.
5) 13,600 tonnes of *D. gahi* (95% CI: 9,974 – 20,355 t) were estimated to remain in the Loligo Box at the end of the 2nd season 2025 (hereafter: escapement biomass). The risk of *D. gahi* escapement biomass being less than 10,000 tonnes at the time of closure was 2.5%.

1. Introduction

The second season (X licence) of the 2025 *Doryteuthis gahi* fishery (Patagonian longfin squid – colloquially *Loligo*) started on July 27th and finished on September 19th following a closure order. Two bad weather days were claimed by the fleet on August 13th and 14th, with no vessels fishing. At the season start, eight X-licensed vessels were required to embark a Marine Mammal Observer (hereafter: MRAG observer) to monitor the presence and incidental capture of pinnipeds. It was anticipated that these observers would embark on the remaining eight vessels of the fleet halfway through the season; this was deferred due to uncertainty surrounding the potential early closure, and eventually, the observers remained on their initial vessels throughout the season. Seal exclusion devices (SEDs) were mandatory for the duration of the season. Ultimately, 0 pinniped mortalities and 1 live release of a South American fur seal *Arctocephalus australis,* were reported for the season.

The total reported *D. gahi* catch under the X licence was 4,967 north + 13,487 south = 18,454 tonnes, corresponding to an average CPUE of 21.8 tonnes per vessel-day. Both total catch and average CPUE were around 20% lower than the long-term average for the 2nd season (Table 1).

Assessment of the Falkland Islands *D. gahi* stock was conducted with depletion time-series models as in previous seasons (Agnew et al. 1998, Roa-Ureta and Arkhipkin 2007, Arkhipkin et al. 2008) and in other squid fisheries (cited in Arkhipkin et al. 2021). Because *D. gahi* has an annual life cycle (Patterson 1988, Arkhipkin 1993), stock cannot be derived from a standing biomass carried over from prior years (Rosenberg et al. 1990, Pierce and Guerra 1994). The depletion model instead calculates an estimate of population abundance over time by evaluating what levels of abundance and catchability must be present to sustain the observed catch rate. Depletion modelling of the *D. gahi* target fishery is used in-season, with

the objective of maintaining an escapement biomass of 10,000 tonnes of *D. gahi* at the season end (Agnew et al. 2002, Barton 2002).

Table 1. *D. gahi* season comparisons since 2004, when the FIFD assumed catch management. Season days: total number of calendar days open to licensed *D. gahi* fishing, including (since 1st season 2013) optional flex days. Vessel days: aggregate number of licensed *D. gahi* fishing days reported by all vessels for the season. Underlined entries are seasons closed by emergency order.

	1st Season			2nd Season		
	Catch (tonnes)	Season days	Vessel days	Catch (tonnes)	Season days	Vessel days
2004	6,668	45	696	18,064	78	1,202
2005	24,773	45	664	29,662	78	1,167
2006	19,056	50	770	23,231	53	817
2007	17,275	50	779	24,239	63	966
2008	24,877	51	780	26,953	78	1,189
2009	12,794	50	773	17,873	59	923
2010	28,681	50	765	36,998	78	1,169
2011	15,288	50	768	18,726	70	1,099
2012	34,727	51	770	35,026	79	1,095
2013	19,906	53	782	19,620	78	1,196
2014	28,117	59	872	19,656	71	1,100
2015	19,424	66	949	10,190	42	665
2016	22,619	68	1,020	23,090	68	1,004
2017	39,425	68	997	24,085	69	1,000
2018	43,086	69	975	35,828	68	977
2019	55,586	68	953	24,748	43	635
2020	29,116	68	1,012	29,759	69	993
2021	59,499	62	891	34,665	68	979
2022	56,080	68	963	43,216	68	982
2023	52,704	67	972	15,513	31	452
2024	47,588	68	974	0	0	0
2025	37,492	58	899	18,454	55	846

2. Methods

2.1. Model updates

The only change to the modelling approach compared to the previous assessment was in the calculation of the catchability prior. This season, the entire fleet fished in the south on the first day of the season, so CPUE data was restricted to the south sub-area. For consistency, data on squid biomass (from the pre-season survey) and average size (from the pre-season survey and the first day of the season) were also limited to the south sub-area when calculating catchability. This differs from the approach in recent years, where biomass and squid size data for the entire Loligo Box were utilised, but is similar to the approach used in some earlier assessments. The effect of this change on model outcomes will depend on the observed catches, i.e. it will be season-specific. Most importantly, the new approach ensures that the catchability prior is consistent with the modelling approach, treating north and south sub-areas as separate stocks.

2.2. Model structure

Stock assessment of *D. gahi* in the Falkland Islands is based on a depletion model. In its basic form (DeLury 1947), a depletion model assumes a closed population in a fixed area for the duration of the assessment. However, the assumption of a closed population is not met in the Falkland Islands fishery, where stock analyses have often shown that *D. gahi* groups arrive in successive waves after the start of the season (Arkhipkin et al. 2021). Arrivals of successive groups are inferred from discontinuities in the CPUE data, as well as biological data, such as size, maturity, and sex ratio. Fishing on a single, closed cohort would be expected to yield gradually decreasing CPUE, but increasing average individual sizes, as the squid grow. If, instead, these data change suddenly, or in contrast to expectation, the immigration of a new group to the population is indicated (Winter and Arkhipkin 2015). To account for immigration events, the population model was formulated as:

$$N_t = \begin{cases} N1 & if\ t = 1 \\ \left(N_{t-1}e^{-\frac{M}{2}} - X_{t-1}\right)e^{-\frac{M}{2}} + N2\ i2_t + N3\ i3_t + \cdots + Nn\ in_t & if\ 1 < t \leq T \end{cases}$$

where N_t is the abundance on day of the season t, *N1* is the initial abundance, *N2:Nn* are abundances of the subsequent in-season immigrations, *i2:in* are dummy variables taking the value of 1 on the day when corresponding immigration occurred and 0 otherwise, X_t is the observed catch in numbers on day of the season t, M is the time-invariant instantaneous natural mortality rate, and T is the duration of the season.

The predicted daily catch in numbers from the population model is expressed as:

$$C_t = qE_tN_te^{-\frac{M}{2}}$$

where q is the catchability coefficient and E_t is the fishing effort on day of the season t. It should be noted that, under the assumption that effort is observed exactly, this could be

transformed into a predicted CPUE by dividing both sides of the equation by effort, without any statistical consequences (Roa-Ureta 2012).

The model is fitted to the observed daily catches in numbers, assuming lognormal distribution of the observations and treating the variance as a nuisance parameter, eliminated by adopting a modified log-likelihood function as an approximation to the exact lognormal log-likelihood function (Roa-Ureta 2012):

$$-LL = \frac{T-2}{2}\log\left(\sum_{t=1}^{T}\left(log(X_t) - log(C_t)\right)^2\right)$$

where X_t and C_t are the observed and predicted catch in numbers on day of the season t, and T is the season duration.

The fishing effort E and observed catch X are assumed to be known without error, and the natural mortality M is treated as a fixed parameter calculated from an empirical equation outside of the model. The number of immigration events and their timing are decided outside of the model and used as fixed inputs. This leaves the catchability q, abundance at the start of the season $N1$, and abundance of the subsequent immigration events $N2{:}Nn$ as free parameters to be estimated. The abundance time-series $N_{1:T}$ is a derived quantity, which can be multiplied by the average individual squid weight time-series to obtain the biomass time-series.

The stock assessment was set in a Bayesian framework, whereby results of the season depletion model are conditioned by prior information on the stock. In this case, the pre-season survey biomass estimate was combined with the CPUE observed on the first day of the season to create an informative lognormal catchability prior, as described in Chapter 5.1. The log-likelihood function of the prior was parameterised as:

$$-LL = log(\sigma) + \frac{1}{2}\left(\frac{log(q) - \mu}{\sigma}\right)^2$$

where q is the catchability estimated by the depletion model, and μ and σ are the mean and standard deviation of the catchability prior in log-space. For prior information on catchability to be relevant, both the survey and the season have to be fishing the same stock with the same gear.

The model was optimised by jointly minimising the negative log-likelihoods from the observations and the prior, using the Nelder-Mead algorithm of the *optim* function in the package *stats* implemented in R version 4.1.3 (R Core Team, 2022). Relative weights in the joint optimisation were assigned to the data and the prior as the converse of their coefficients of variation (CV), calculated as described in Chapter 5.2. The estimated parameter values presented in the report are maximum posterior density (MPD) point estimates, and the associated 95% credible intervals are calculated from the parameter marginal posterior distributions.

The marginal posterior distributions of the parameters in Bayesian analysis were computed using a Markov Chain Monte Carlo (MCMC) method (Gamerman and Lopes 2006). For each tested model, three chains were run: one chain initiated with the MPD parameter estimates, one chain initiated with these parameter estimates ×2, and one chain initiated with these parameter estimates ×¼. Each chain was run for 210,000 iterations; the first 10,000 iterations were discarded as burn-in sections, and the subsequent 200,000 iterations were

thinned by a factor of 100 to reduce autocorrelation; the resulting 2,000 values approximate the Bayesian posterior distribution. Individual chains were investigated for evidence of non-convergence using trace plots, chain autocorrelation plots, stationarity test (Geweke 1992), and stationarity and half-width tests (Heidelberger and Welch 1983). Convergence of the three chains for each parameter was tested using Gelman and Rubin's diagnostic $\hat{R}$, based on a comparison of within-chain and between-chain variances (Brooks and Gelman 1998). When convergence was satisfied, the three chains were combined as one final set.

Depletion models were fitted separately for the north and south sub-areas of the Loligo Box fishing zone, as *D. gahi* sub-stocks emigrate from different spawning grounds and remain to an extent segregated (Arkhipkin and Middleton 2002), even though they represent a single intermixed population (Shaw et al. 2004). The *q* prior was calculated based on the south sub-area, as the entire fleet fished in the south on the first day of the season. The same prior was then used in depletion models for the north and south sub-areas (for details on prior calculation, see Chapter 5.1).

Total escapement biomass was defined as the aggregate biomass of *D. gahi* on the last day of the season for north and south sub-areas combined, with north and south posterior distributions added together randomly to obtain a 95% credible interval on escapement.

Natural mortality

Natural mortality was parameterised in the depletion model as a time-invariant instantaneous rate, calculated from the Hamel and Cope (2022) longevity-based estimator $M = 5.40 / A_{max}$, with a corresponding log-space prediction error = 0.31 (or CV = 32%; Maunder et al. 2023). Assuming a maximum age A_{max} = 352 days for *D. gahi* resulted in a mortality rate estimate $M = 0.0153$ day^{-1}.

Immigration peaks

The start days of immigration (arrivals of new *D. gahi* groups) are hereafter referred to as immigration peaks. By definition, squid present on the first day of the season is considered the first immigration peak, even though this is de facto not an in-season immigration. Each immigration peak marks the start of a new depletion period, as the squid that immigrated are being removed by fishing and natural mortality.

Immigration peaks were inferred from changes in trends of the CPUE, sex ratio, maturity, and average individual squid size. CPUE was calculated in metric tonnes of *D. gahi* caught per vessel-day. Days were used rather than trawl hours as the basic unit of effort. Commercial vessels do not trawl standardised duration hours, but rather durations that best suit their daily processing requirements. An effort index of days is therefore more consistent (FIFD 2004, Winter and Arkhipkin 2015). Inclusion of additional immigration peaks was also partially evaluated by improvement of the Akaike information criterion (AIC; Akaike 1973), when changes in CPUE, sex proportions, maturity, and sizes were ambiguous.

Average individual weights

Daily average individual weight is obtained from the length-weight conversion of mantle lengths measured in-season by FIFD and MRAG observers. To smooth day-to-day fluctuations, Generalised Additive Model (GAM) trends were fitted to daily average individual weights per haul, weighted by sample size, and used whenever converting abundance to biomass. North and south sub-areas were calculated separately. For continuity, GAMs were fitted using both the pre-season survey and in-season data.

2.3. Data

Data collection

Fishery self-reporting data were extracted from the electronic logbooks and included catch per haul with the corresponding time, position, and depth at the start/end of each haul. During the season, four FIFD fishery observers were deployed on four vessels for 75 sampling days (not counting seabird observation days) (Desmet 2025, Minichino 2025, Orlandi 2025, Villarroel 2025). Of the 53 fishing days of the season, one day had no FIFD fishery observer sampling, 29 days had one FIFD fishery observer sampling, and 23 days had two FIFD fishery observers sampling. Except for seabird days, FIFD fishery observers were tasked with sampling 200 *D. gahi* at two stations daily and reporting their maturity stages, sex, and lengths to 0.5 cm. Additionally, each FIFD fishery observer reported individual weights of 200 *D. gahi* twice a week. MRAG observers were tasked with measuring 100 unsexed lengths of *D. gahi* per day.

Commercial catch and effort data

846 vessel-days were fished during the season, with a median of 16 vessels per day (mean 15.4). The north sub-area was fished on 40 out of 53 fishing days, for 26.9% of total catch (4,966.5 tonnes *D. gahi*) and 32.3% of effort (273 vessel-days). The south sub-area was fished on 52 out of 53 fishing days, for 73.1% of total catch (13,487.5 tonnes *D. gahi*) and 67.7% of effort (573 vessel-days) (Figures 1 and 2).

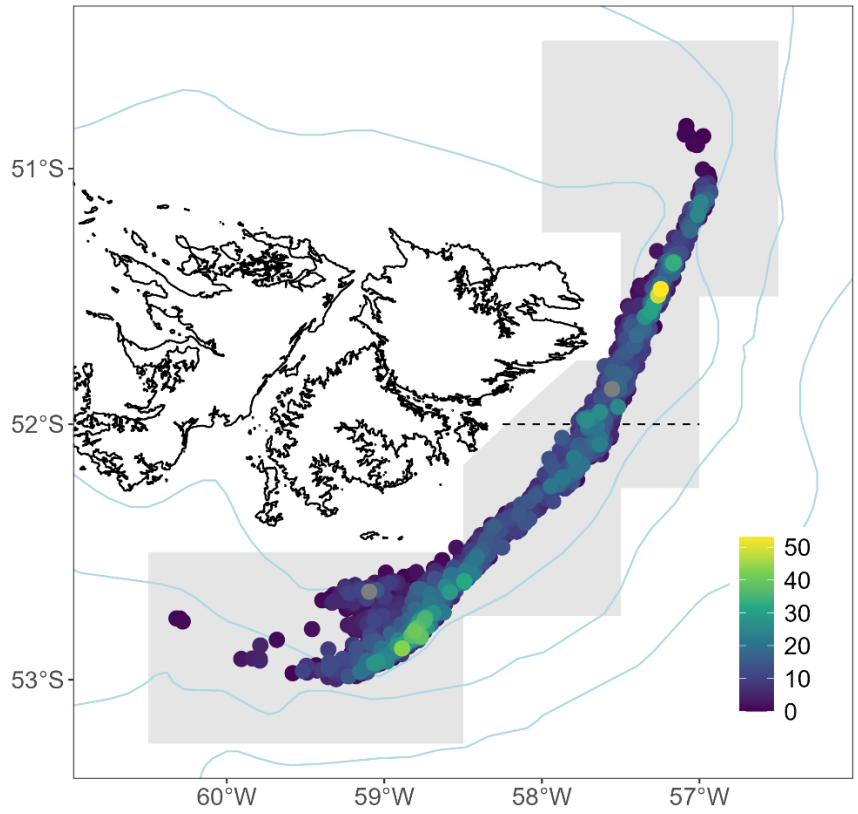

Figure 1. Spatial distribution of trawls (mean coordinate positions) during the 2nd season 2025, colour-scaled to *D. gahi* catch weight (max = 53.1 tonnes). 2,414 trawl catches were taken during the season. Grey shading denotes the Loligo Box fishing zone. Dashed line marks the boundary between north and south sub-areas (52°S parallel).

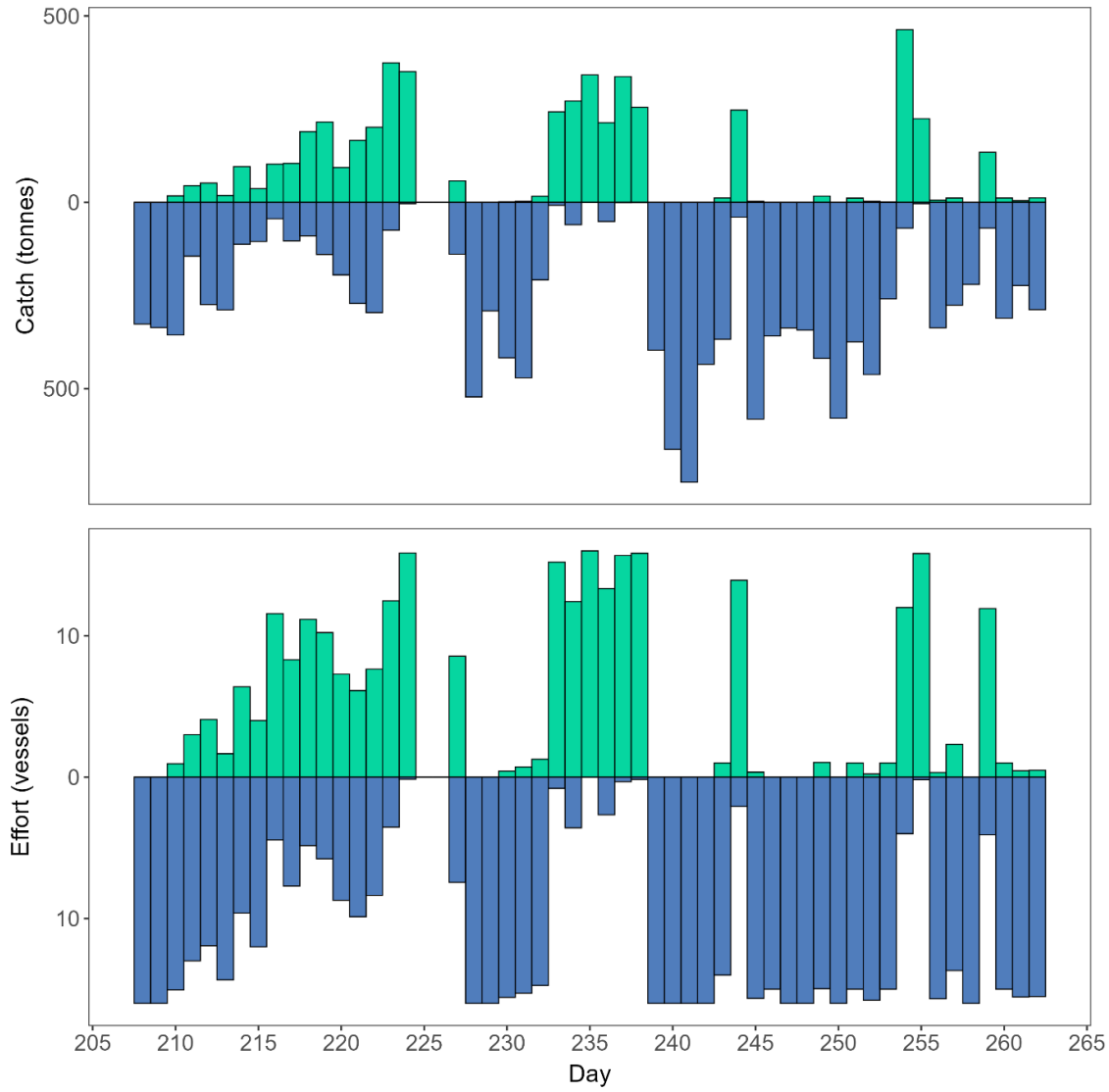

Figure 2. Daily *D. gahi* catch and effort distribution by assessment sub-area north (green) and south (blue) during the 2nd season 2025. The season started on July 27th (chronological day 208) and finished on September 19th (chronological day 262) following a closure order.

Length-weight data

The length-weight relationship was calculated as $W = a\,ML^b$, based on the mantle length (cm) and body weight (g) data collected during the 2nd season 2025, supplemented by data from the surveys done in the 2nd season 2024, because 2025 data became available progressively throughout the season. The final dataset for the length-weight relationship included 2,032 measures from 2024 and 5,876 measures from 2025, with estimated parameters a = 0.143 and b = 2.262.

3. Results

3.1. Immigration peaks

Two days in each sub-area were identified as representing the onset of significant immigration throughout the season. The first immigration peak was set on the same day in both areas by design (the first day of the season). Coincidentally, the second immigration peak was also inferred to have occurred on the same date in the two sub-areas.

In the north sub-area, commercial fishing began on day 210 (July 29th) with three vessels each making one haul. Initially low CPUE (<20 t/vessel-day) further declined during the first week of the fishery to less than 10 t/vessel-day. This was followed by an increasing CPUE trend during the second week, culminating in a 3-day CPUE peak of around 30 t/vessel-day (Figure 3). Consequently, an immigration peak was inferred around the midpoint of the CPUE increase (day 218). For the rest of the season, the CPUE trend fluctuated widely, partly due to several days with very low fishing effort (few vessels fishing, sometimes only for a few hours), which may have led to CPUE figures that were not necessarily representative. The two CPUE outliers associated with high effort (10+ vessels fishing) were recorded on days 227 (low CPUE) and 254 (high CPUE). The low CPUE on day 227 could have been caused by bad weather on the two previous days, leading to squid dispersal. The high CPUE on day 254 was indicative of immigration; however, the CPUE dropped sharply the next day and remained low, suggesting that this was only a local aggregation of squid rather than a substantial immigration. Therefore, a two-immigration peak model (days 208 and 218) was preferred for the north sub-area.

In the south sub-area, commercial fishing began on day 208 (July 27th) with 16 vessels. The CPUE trend was similar to that in the north during the first two weeks of the season (decreasing during the first and increasing during the second week). Consequently, an immigration peak was inferred to have occurred on the same date as in the north, around the midpoint of the CPUE increase (day 218). For the rest of the season, the most prominent feature of the CPUE trend was a drop on days 237-238, followed by a sharp increase on days 241-241. The drop on days 237-238 was based on very low fishing effort (one vessel on each day), which may have led to CPUE figures that were not necessarily representative. The increase on days 240-241 was indicative of immigration; however, the CPUE dropped by half in the following two days in the same location, suggesting either a small immigration or local aggregation. Analysis of the biological data showed that the increase in CPUE was associated with an increase in squid size and maturity (Figure 5), contrary to the expectation in the case of new immigration (younger, less mature squid). Therefore, this was not considered an immigration in the base-case scenario, although it was explored as an alternative scenario during the in-season modelling. Given the above, a two-immigration peak model (days 208 and 218) was preferred for the south sub-area.

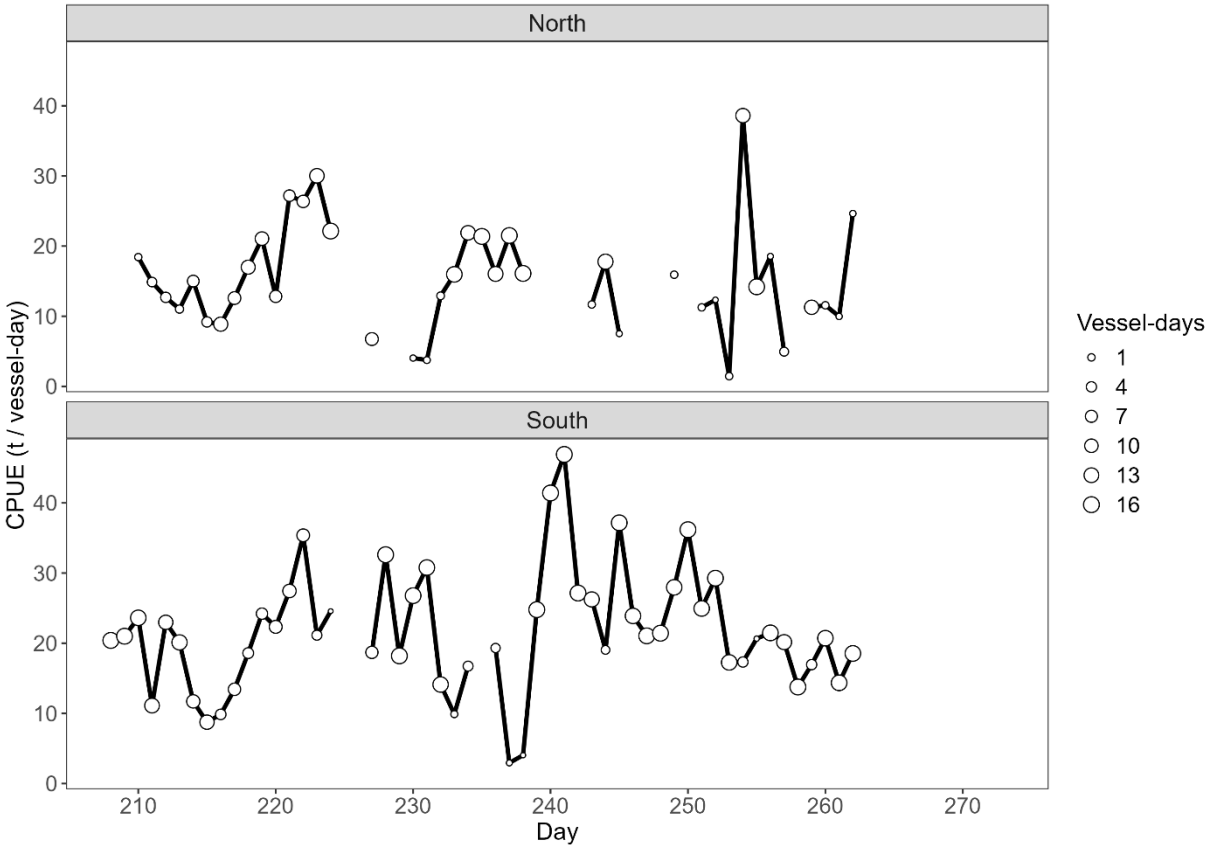

Figure 3. *D. gahi* CPUE time-series in the north and south sub-areas during the 2nd season 2025. Dot sizes are proportionate to the number of vessels fishing. Line segments join data from consecutive days.

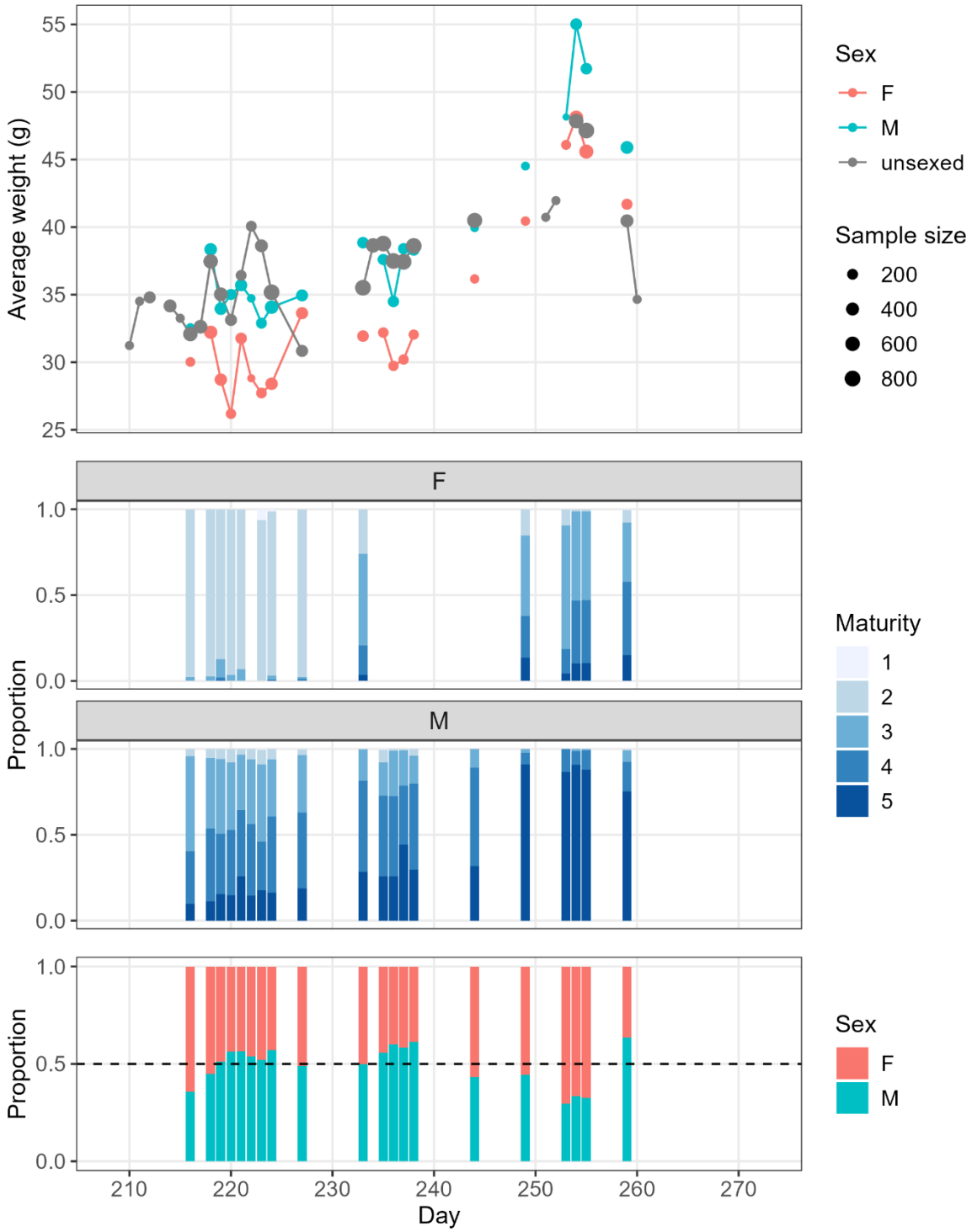

Figure 4. *D. gahi* biological data time-series in the north sub-area during the 2nd season 2025. Average individual weights by sex, proportion of maturity stages per sex, and proportion of sexes are from the FIFD observer data. The average weights of unsexed individuals are from the MRAG observer data.

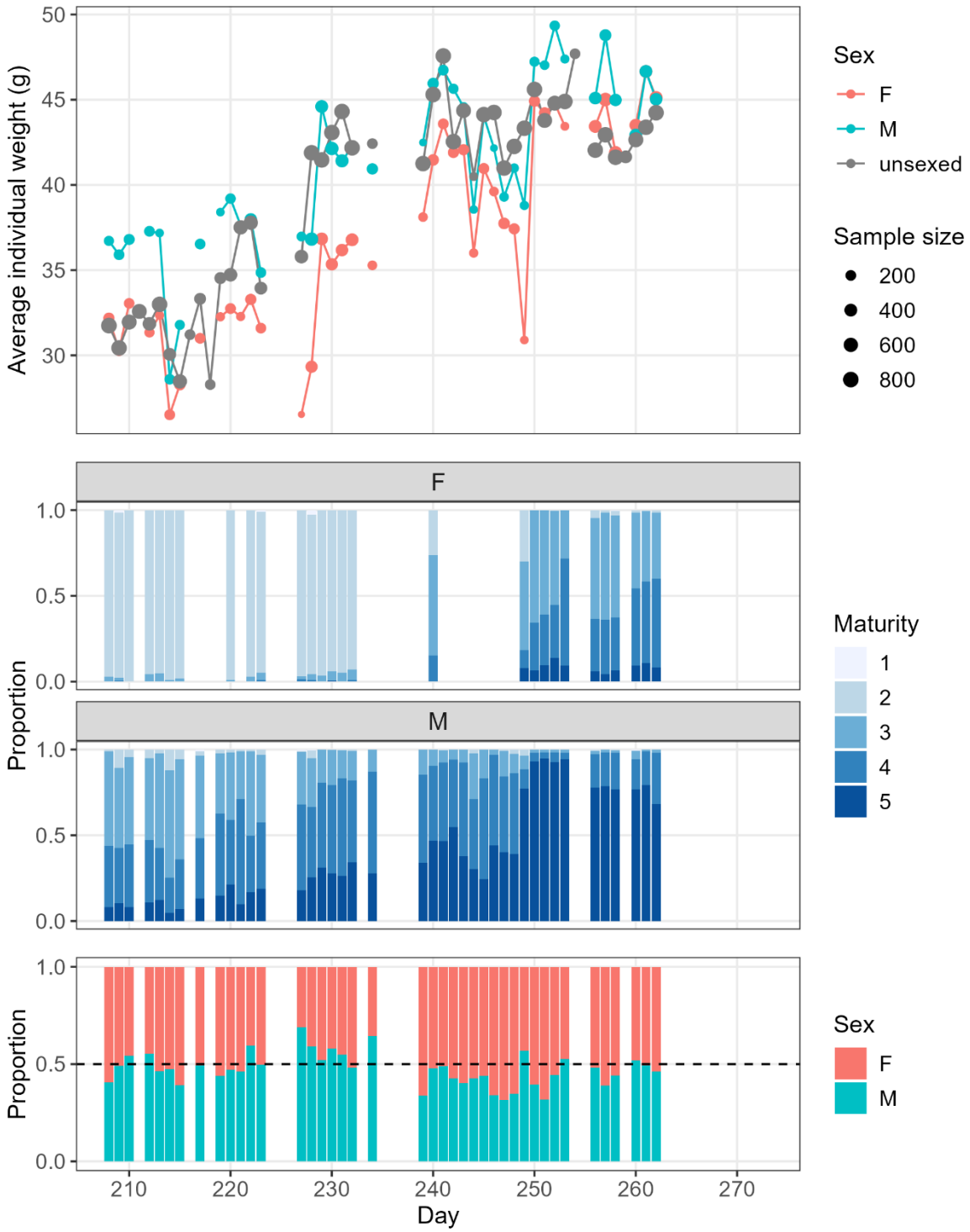

Figure 5. *D. gahi* biological data time-series in the south sub-area during the 2nd season 2025. Average individual weights by sex, proportion of maturity stages per sex, and proportion of sexes are from the FIFD observer data. The average weights of unsexed individuals are from the MRAG observer data.

3.2. Average individual weights

GAMs fitted to daily average individual weights showed similar levelled trends in the north and south sub-areas during the survey and first two weeks of the season, with average sizes in the range 32-35 g. In the south, this was followed by a size increase in mid-season (days 220-240) and a more levelled trend afterwards. In the north, the increase in size appeared slower, although it reached a similar level as in the south towards the end of the season, in the range 44-45 g (barring the last week, when very little data was available for the area) (Figure 6). It should be noted that the perceived trends reflect not only squid growth, but also immigration (e.g., an influx of smaller squid than previously found in the area) and the spatial distribution of the fleet (shifting the effort to shallower or deeper waters, where different sizes of squid may be available).

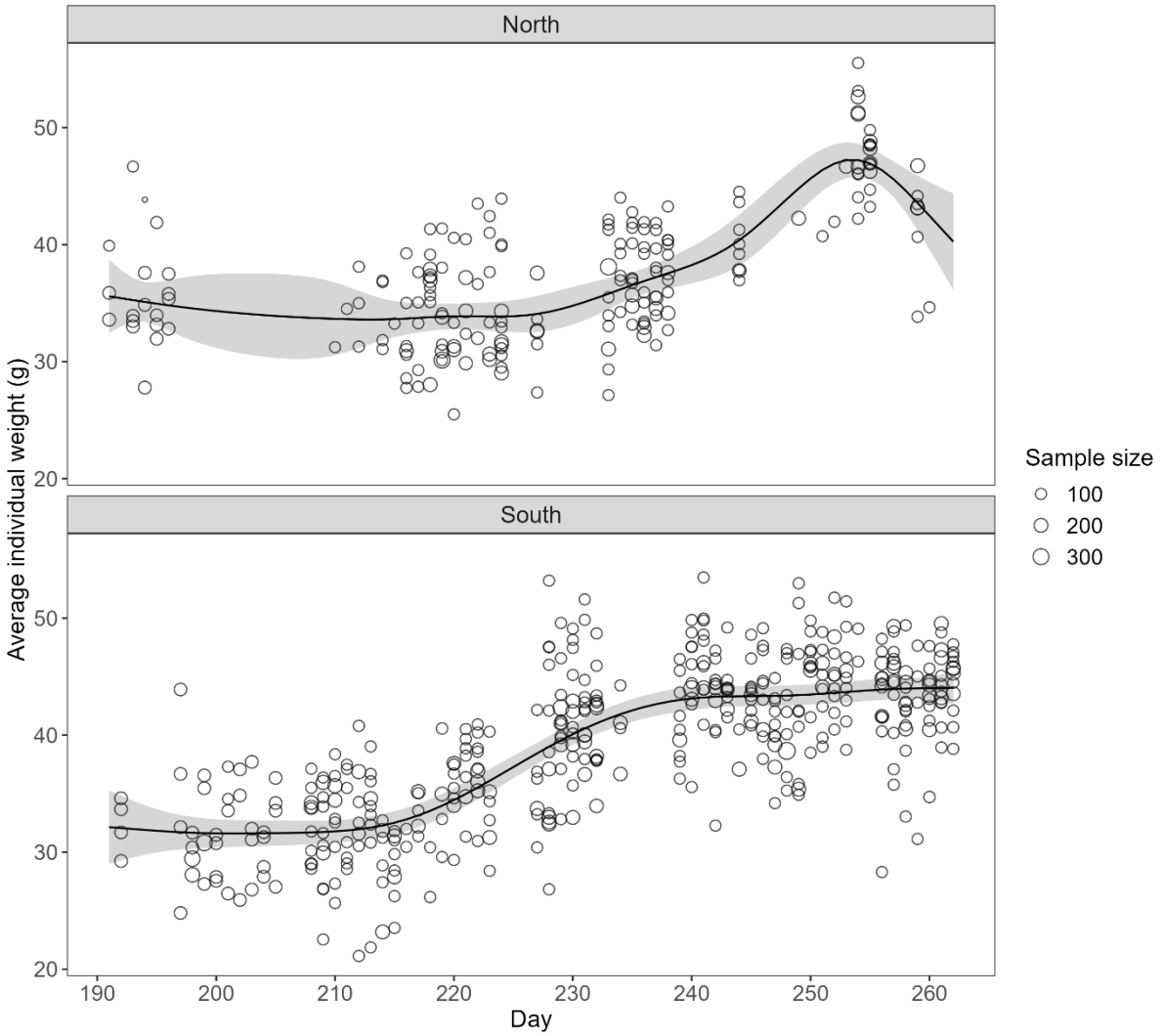

Figure 6. Average individual *D. gahi* weights per haul from FIFD and MRAG observer data (circles) and the fitted GAM trend (black line) with 95% confidence interval (grey shading).

3.3. Depletion model – north sub-area

Model fit

For the north sub-area, the model fitted the observed catches reasonably well; noting that catches were sparse in the second half of the season (Figure A.1). MPD parameter estimates (catchability *q*, numbers of squid present on the first day of the season *N1* and immigrating on the subsequent immigration event *N2*) and MCMC samples from the posterior distribution are given in Appendix (Chapter 5.4, Figure A.2).

MCMC trace plots showed no evident lack of convergence in estimated parameters (Figure A.4). All the MCMC diagnostic tests were passed by the estimated parameters, indicating convergence (Table A.1, Table A.2). No autocorrelation in MCMC samples was observed (Figure A.5).

Biomass estimates

In the north sub-area, the model estimated biomass for the first day of the season (July 27th) at 9,287 t (95% CI: 5,568 – 17,002 t); not significantly different from the pre-season survey biomass estimate of 7,464 t (95% CI: 4,281 – 15,818 t) (Figure 7). For the final day of the season (September 19th), estimated *D. gahi* escapement biomass north was 5,385 t (95% CI: 3,592 – 8,721 t) (Figure 8). The highest estimated biomass of the season occurred with the second immigration peak on day 218, reaching 14,163 t (Figure 9).

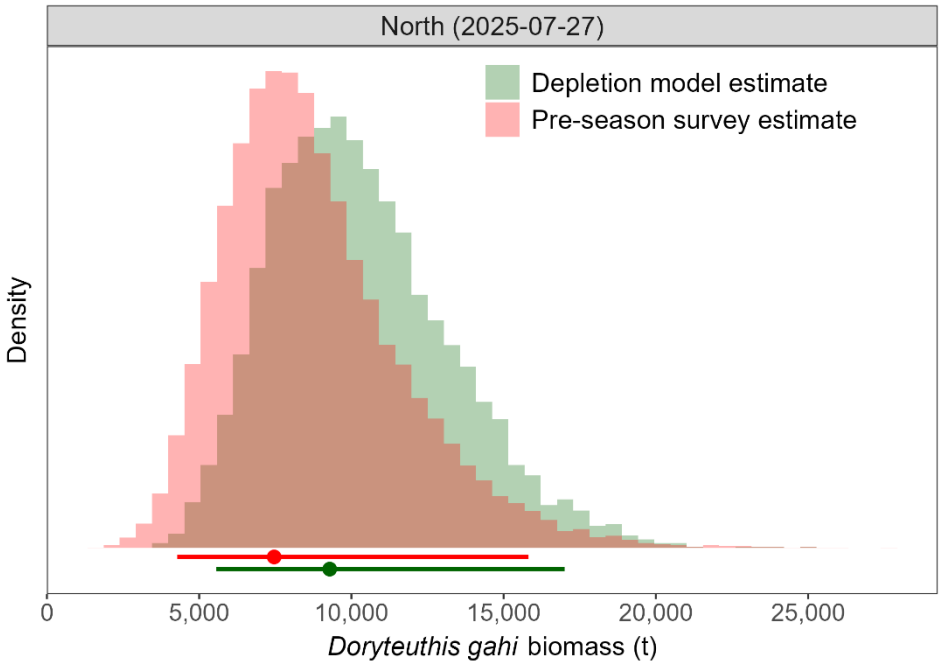

Figure 7. *D. gahi* biomass estimate from the pre-season survey (red histogram, dot, and line: bootstrapped distribution, MLE estimate, and 95% confidence interval, respectively) and biomass estimate on the first day of the season from the depletion model (green histogram, dot, and line: MCMC posterior distribution, MPD estimate, and 95% credible interval, respectively)

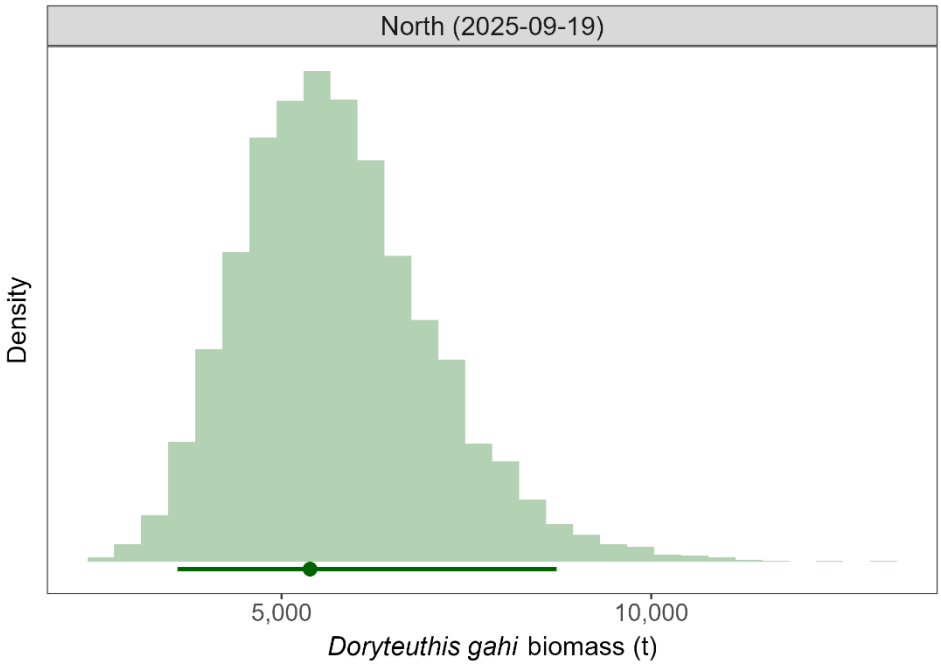

Figure 8. Posterior distribution of *D. gahi* escapement biomass in the north sub-area, at the end of the season. Green dot and line: MPD estimate and 95% credible interval.

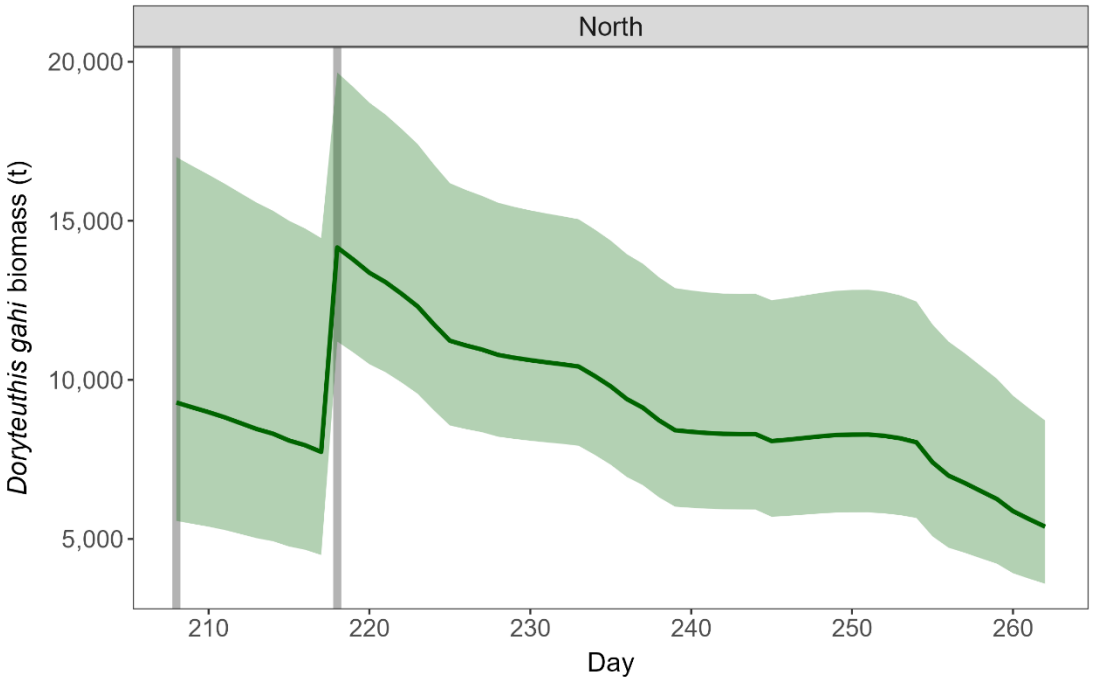

Figure 9. Time series of *D. gahi* biomass estimates in the north sub-area throughout the season. Green line and shading: MPD estimate and 95% credible interval. Grey bars: immigration peaks north (days 208 and 218).

3.4. Depletion model – south sub-area

Model fit

For the south sub-area, the model fitted the observed catches reasonably well for the first five weeks of the season and poorly for the last three weeks (Figure A.1). The poor fit to the observed catches over the last three weeks was alleviated when additional immigration was assumed to have occurred just before it (tested as an alternative scenario). However, this led to a poorer fit to the mid-season data, and additional immigration had no substantive support in the biological data. MPD parameter estimates (catchability *q*, numbers of squid present on the first day of the season *N1* and immigrating on the subsequent immigration event *N2*) and MCMC samples from the posterior distribution are given in Appendix (Chapter 5.4, Figure A.3).

MCMC trace plots showed no evident lack of convergence in estimated parameters (Figure A.6). All the MCMC diagnostic tests were passed by all the estimated parameters, indicating convergence (Table A.3, Table A.4). No autocorrelation in MCMC samples was observed (Figure A.7).

Biomass estimates

In the south sub-area, the model estimated biomass for the first day of the season (July 27th) at 13,132 t (95% CI: 8,504 – 24,650 t), not significantly different from the pre-season survey biomass estimate of 14,231 t (95% CI: 11,351 – 18,874 t) (Figure 10). For the final day of the season (September 19th), estimated *D. gahi* escapement biomass south was 8,215 t (95% CI: 5,034 – 14,101 t) (Figure 11). The highest estimated biomass of the season occurred with the second immigration peak on day 218, reaching 25,295 t (Figure 12).

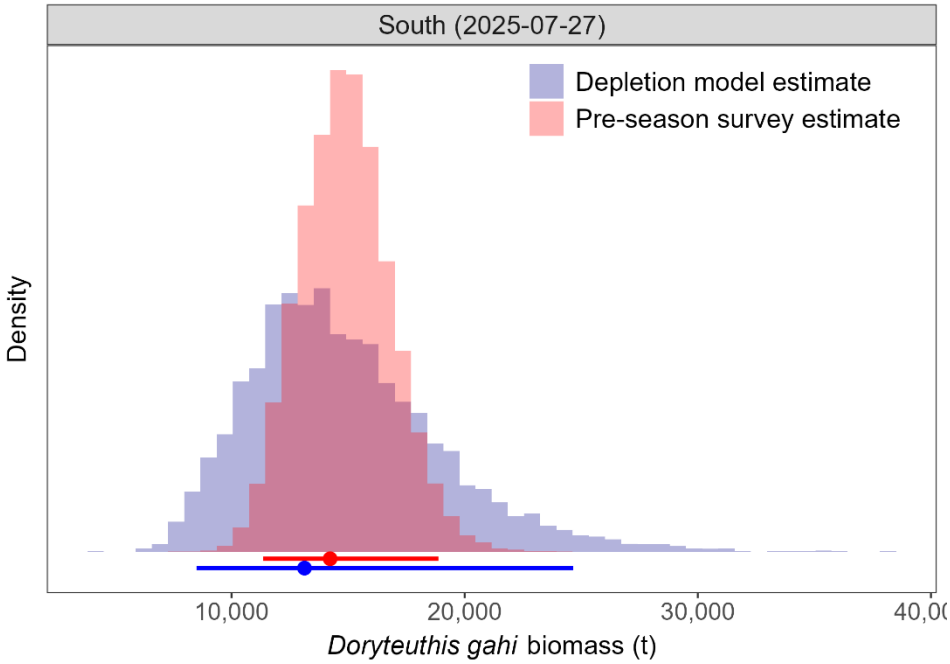

Figure 10. *D. gahi* biomass estimate from the pre-season survey (red histogram, dot, and line: bootstrapped distribution, MLE estimate, and 95% confidence interval, respectively) and biomass estimate on the first day of the season from the depletion model (blue histogram, dot, and line: MCMC posterior distribution, MPD estimate, and 95% credible interval, respectively)

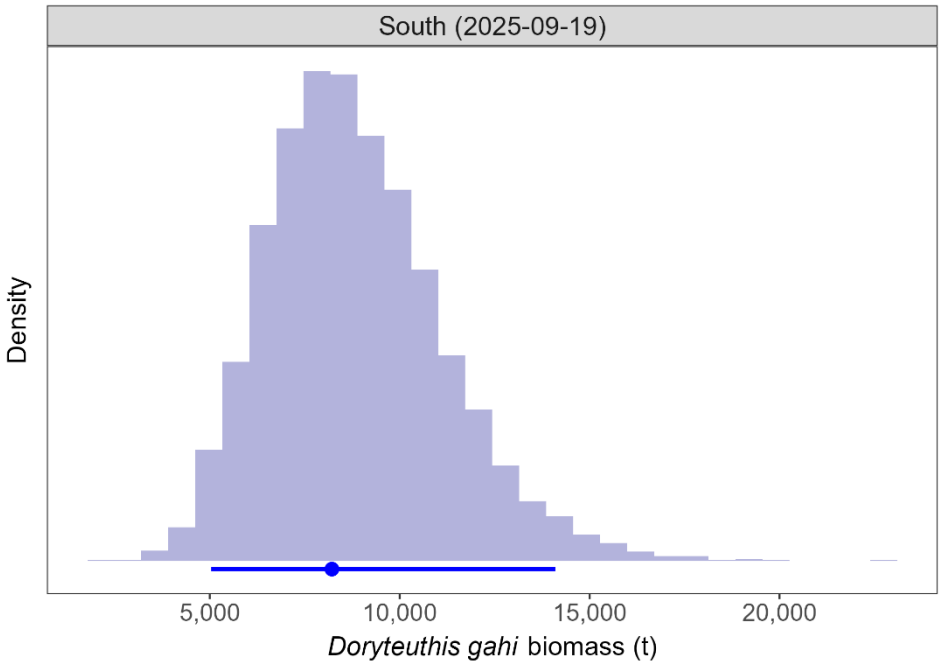

Figure 11. Posterior distribution of *D. gahi* escapement biomass in the south sub-area, at the end of the season. Blue dot and line: MPD estimate and 95% credible interval.

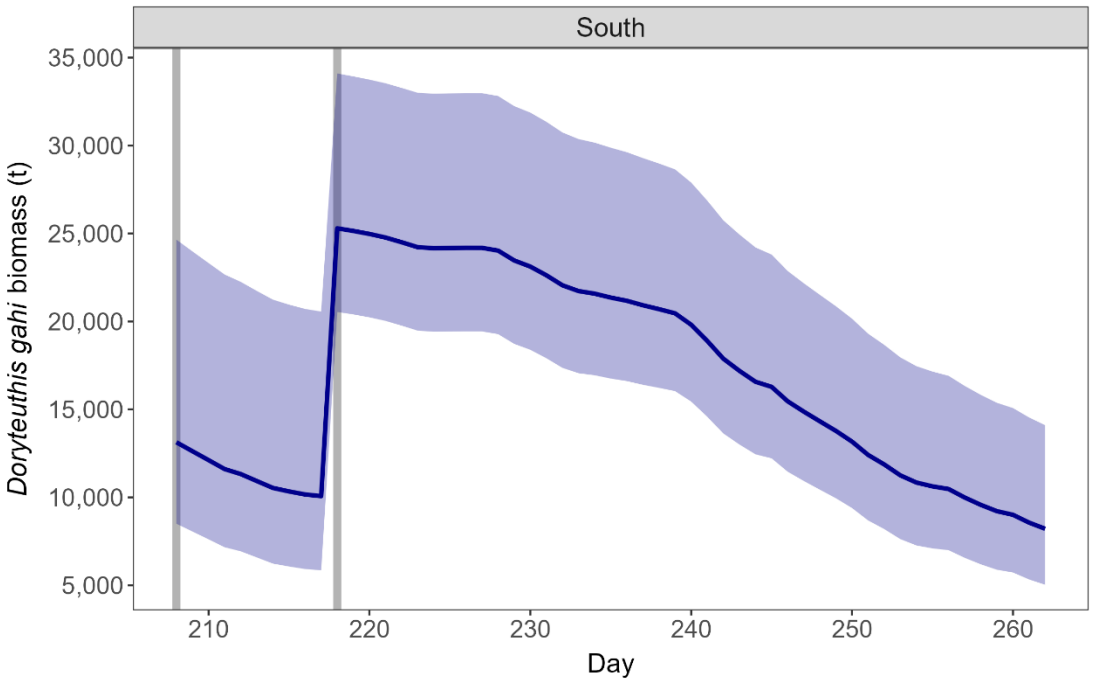

Figure 12. Time series of *D. gahi* biomass estimates in the south sub-area throughout the season. Blue line and shading: MPD estimate and 95% credible interval. Grey bars: immigration peaks south (days 208 and 218).

3.4. Immigration

The size of *D. gahi* immigration on selected immigration days was inferred by how many more squid were estimated present than the day before, minus the number caught and the number expected to have died naturally:

$$I_{t,a} = N_{t,a} - \left(N_{t-1,a}e^{-M/2} - X_{t-1,a}\right)e^{-M/2}$$

where *I* is the immigration in numbers, *N* is the abundance estimated in the depletion model, *X* is the observed catch, *M* is the instantaneous natural mortality, *t* is the selected immigration day, and *a* is the sub-area. Immigration biomass was then calculated by multiplying the immigration numbers by the average individual *D. gahi* weight on the day of immigration. Credible intervals of the immigration estimates were calculated by applying the above equation to the MCMC iterations of the depletion models.

In the current assessment, an immigration peak was identified on day 218 for both sub-areas (initial abundance on day 208 was de facto not an in-season immigration). The resulting *D. gahi* immigration on day 218 was 6,636 t (95% CI: 1,139 – 11,755 t) in the north and 15,366 t (95% CI: 5,879 – 22,885 t) in the south sub-area. Total (north + south) immigration, with credible interval calculated from the randomised addition of the north and south estimate distributions, was 22,002 t (95% CI: 10,981 – 30,770 t).

3.5. Escapement biomass

Total escapement biomass was defined as the aggregate biomass of *D. gahi* at the end of day 262 (September 19th) for the combined north and south sub-areas. Total *D. gahi* escapement biomass, with credible interval calculated from the randomised addition of the north and south posterior distributions, was 13,600 t (95% CI: 9,974 – 20,355 t) (Figure 13). The risk of the escapement biomass being below the conservation threshold of 10,000 tonnes at the time of season closure was 2.5% (calculated as the proportion of the total escapement biomass distribution below the threshold).

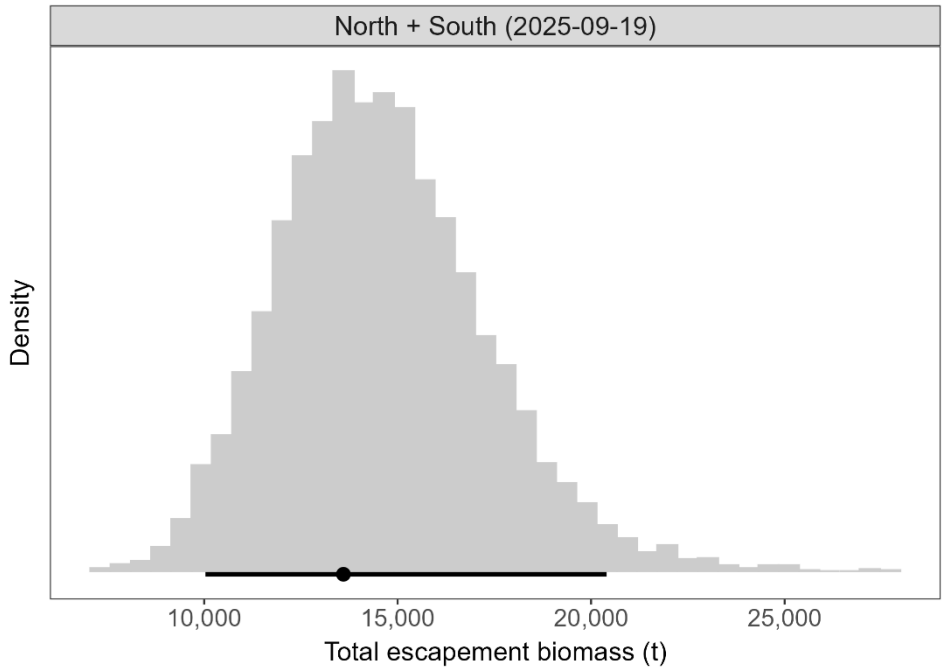

Figure 13. Combined posterior distribution of *D. gahi* escapement biomass north and south at the season end (September 19th). Black dot and line: MPD estimate and 95% credible interval.

3.6. Fishery bycatch

From 846 vessel-days of the season, 840 reported *D. gahi* squid as their primary catch. The remaining six vessel-days had large catches of common hake *Merluccius hubbsi* (8 - 30 tonnes, 58 - 79% of the total daily catch). *D. gahi* represented 93.2% of the season total catch.

The highest aggregate bycatches in the 2nd season 2025 were common hake HAK *M. hubbsi* with 716 tonnes from 775 vessel-days (catch reports), common rock cod PAR *Patagonotothen ramsayi* (370 t, 806 v-days), scallop ZYP *Zygochlamys patagonica* (101 t, 705 v-days), jellyfish MED Scyphozoa (29 t, 457 v-days), black southern rock cod PTE *Patagonotothen tessellata* (28 t, 353 v-days), frogmouth CGO *Cottoperca gobio* (22 t, 725 v-days), starfish AST Asteroidea (11 t, 153 v-days), and skate RAY Rajiformes (11 t, 673 v-days). Bycatch distributions by grid square are shown in Figure 14; the complete catch composition is in Table A.5.

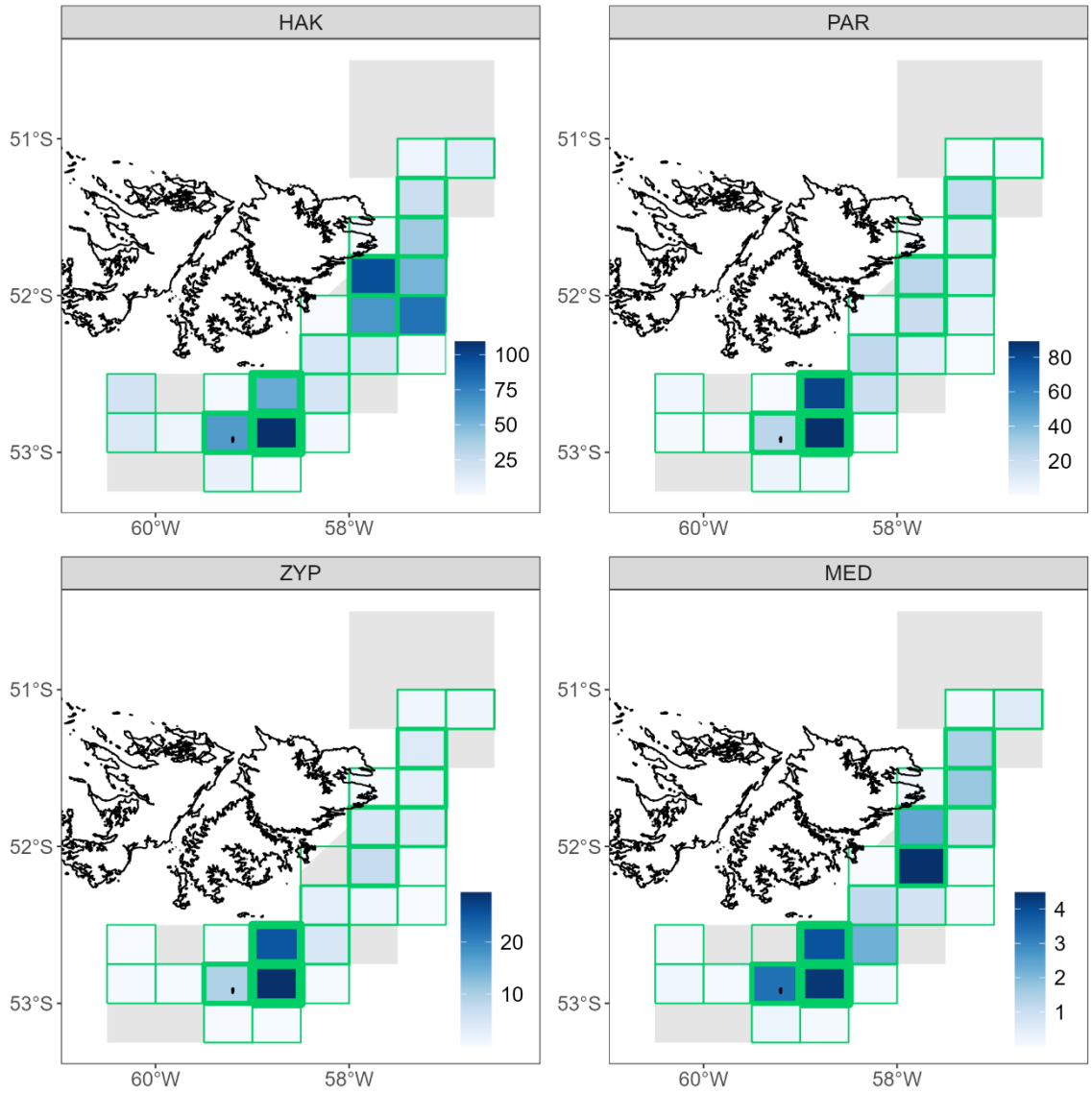

Figure 14. Distributions of the eight main bycatch species catches by grid square in the 2nd season 2025. Thickness of grid lines is proportional to the number of vessel-days (1 to 187 per grid square; 24 unique grid squares were occupied). Blue-scale is proportional to bycatch weight (tonnes).

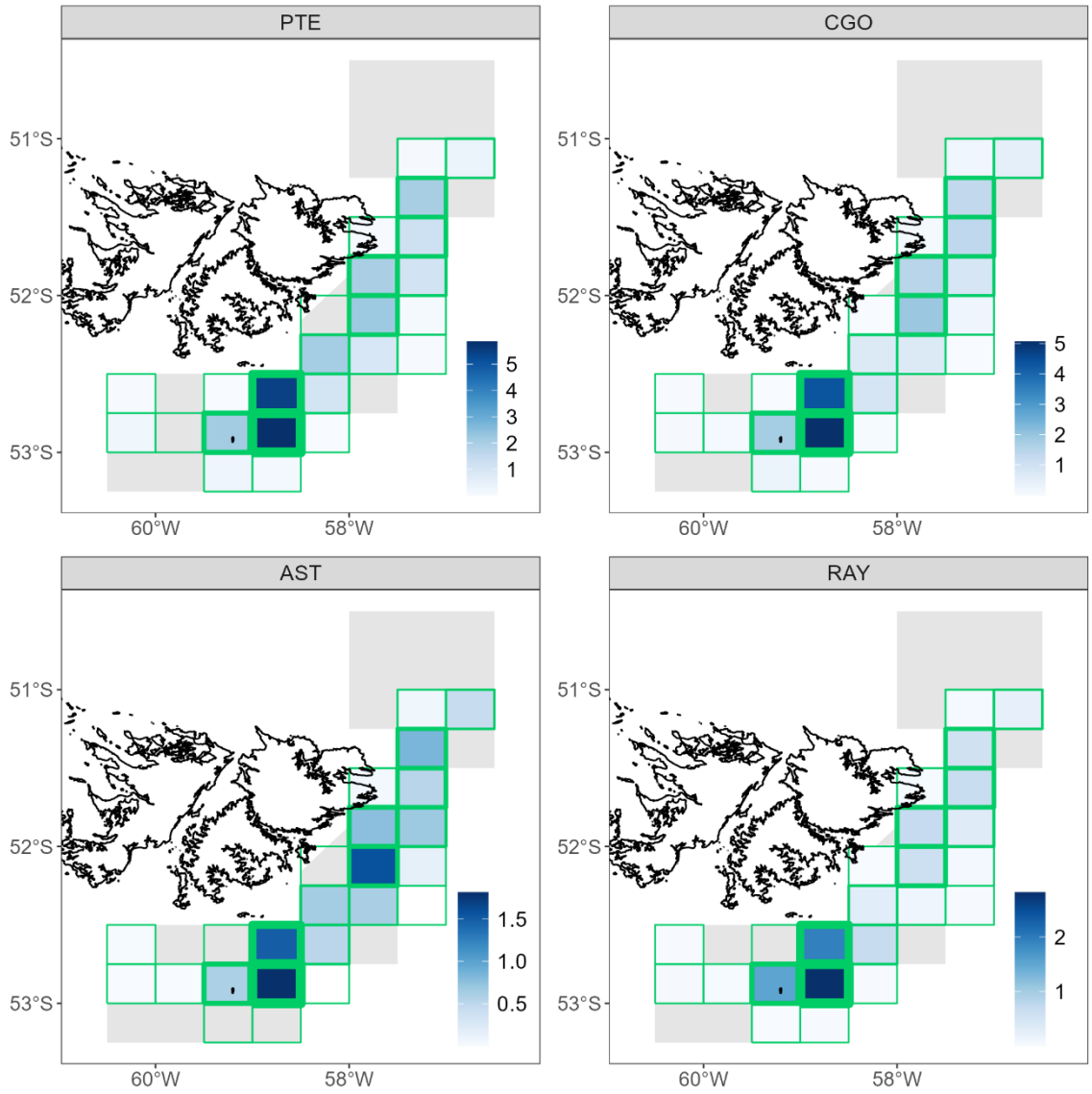

Figure 14. Continued.

4. References

Agnew DJ, Baranowski R, Beddington JR, des Clers S, Nolan CP. 1998. Approaches to assessing stocks of *Loligo gahi* around the Falkland Islands. Fisheries Research 35: 155-169.

Agnew DJ, Beddington JR, Hill S. 2002. The potential use of environmental information to manage squid stocks. Canadian Journal of Fisheries and Aquatic Sciences 59: 1851-1857.

Akaike H. 1973. Information theory and an extension of the maximum likelihood principle. 2nd International Symposium on Information Theory: 267-281.

Arkhipkin A. 1993. Statolith microstructure and maximum age of *Loligo gahi* (Myopsida: Loliginidae) on the Patagonian Shelf. Journal of the Marine Biological Association of the UK 73: 979-982.

Arkhipkin AI, Hendrickson LC, Payá I, Pierce GJ, Roa-Ureta RH, Robin J-P, Winter A. 2021. Stock assessment and management of cephalopods: advances and challenges for short-lived fishery resources. ICES Journal of Marine Science 78: 714-730.

Arkhipkin AI, Middleton DAJ, Barton J. 2008. Management and conservation of a short-lived fishery resource: *Loligo gahi* around the Falkland Islands. American Fisheries Society Symposium 49: 1243-1252.

Arkhipkin AI, Middleton DAJ. 2002. Sexual segregation in ontogenetic migrations by the squid *Loligo gahi* around the Falkland Islands. Bulletin of Marine Science 71: 109-127.

Barton J. 2002. Fisheries and fisheries management in Falkland Islands Conservation Zones. Aquatic Conservation: Marine and Freshwater Ecosystems 12: 127-135.

Brooks SP, Gelman A. 1998. General methods for monitoring convergence of iterative simulations. Journal of Computational and Graphical Statistics 7: 434-455.

DeLury DB. 1947. On the estimation of biological populations. Biometrics 3: 145-167.

Desmet L. 2025. Observer Report 1443. Technical Document, FIG Fisheries Department. 33 p.

FIFD. 2004. Fishery Report, *Loligo gahi*, Second Season 2004. Fishing statistics, biological trends, and stock assessment. Technical Document, FIG Fisheries Department. 15 p.

Gamerman D, Lopes HF. 2006. Markov Chain Monte Carlo. Stochastic simulation for Bayesian inference. 2nd edition. Chapman & Hall/CRC.

Geweke J. 1992. Evaluating the accuracy of sampling-based approaches to calculating posterior moments. In: Bernardo JM, Berger JO, David AP, Smith AFM (Eds.). Bayesian Statistics, 4. Clarendon Press, Oxford, 169-194.

Hamel OS, Cope JM. 2022. Development and considerations for application of a longevity-based prior for the natural mortality rate. Fisheries Research 256: 106477.

Heidelberger P, Welch P. 1983. Simulation run length control in the presence of an initial transient. Operations Research 31: 1109-1144.

Maunder MN, Hamel OS, Lee H-H, Piner KR, Cope JM, Punt AE, Ianelli JN, Castillo-Jordan C, Kapur MS, Methot RD. 2023. A review of estimation methods for natural mortality and their performance in the context of fishery stock assessment. Fisheries Research 257: 106489.

Minichino R. 2025. Observer Report 1449. Technical Document, FIG Fisheries Department. 27 p.

Orlandi N. 2025. Observer Report 1448. Technical Document, FIG Fisheries Department. 33 p.

Patterson KR. 1988. Life history of Patagonian squid *Loligo gahi* and growth parameter estimates using least-squares fits to linear and von Bertalanffy models. Marine Ecology Progress Series 47: 65-74.

Payá I. 2010. Fishery Report. *Loligo gahi*, Second Season 2009. Fishery statistics, biological trends, stock assessment and risk analysis. Technical Document, FIG Fisheries Department. 54 p.

Pierce GJ, Guerra A. 1994. Stock assessment methods used for cephalopod fisheries. Fisheries Research 21: 255-285.

R Core Team. 2022. R: A language and environment for statistical computing. R Foundation for Statistical Computing, Vienna, Austria. http://www.R-project.org/

Roa-Ureta R, Arkhipkin AI. 2007. Short-term stock assessment of *Loligo gahi* at the Falkland Islands: sequential use of stochastic biomass projection and stock depletion models. ICES Journal of Marine Science 64: 3-17.

Roa-Ureta R. 2012. Modelling in-season pulses of recruitment and hyperstability-hyperdepletion in the *Loligo gahi* fishery around the Falkland Islands with generalized depletion models. ICES Journal of Marine Science 69: 1403-1415.

Rosenberg AA, Kirkwood GP, Crombie JA, Beddington JR. 1990. The assessment of stocks of annual squid species. Fisheries Research 8: 335-350.

Shaw PW, Arkhipkin AI, Adcock GJ, Burnett WJ, Carvalho GR, Scherbich JN, Villegas PA. 2004. DNA markers indicate that distinct spawning cohorts and aggregations of Patagonian squid, *Loligo gahi*, do not represent genetically discrete subpopulations. Marine Biology 144: 961-970.

Villarroel M. 2025. Observer Report 1445. Technical Document, FIG Fisheries Department. 28 p.

Winter A, Arkhipkin A. 2015. Environmental impacts on recruitment migrations of Patagonian longfin squid (*Doryteuthis gahi*) in the Falkland Islands with reference to stock assessment. Fisheries Research 172: 85-95.

5. Appendix

5.1. Catchability prior

The catchability coefficient *q* for the season was defined as the ratio of *D. gahi* observed CPUE (in numbers per vessel-day) and estimated abundance on the first fishing day of the season (day 208):

$$\hat{q} = \frac{CPUE(N)_{208}}{\widehat{N}_{208}}$$

It should be noted that all vessels fished in the south sub-area on the first day of the season. Therefore, only observations and estimates for the south sub-area (i.e. CPUE, abundance, and average squid weight) were used to construct the catchability prior.

The CPUE in numbers per vessel-day was obtained by dividing the observed CPUE in biomass per vessel-day (reported by the fishery) by the GAM-predicted individual squid weight on the first day of the season:

$$CPUE(N)_{208} = \frac{CPUE(B)_{208}}{\widehat{w}_{208}}$$

The abundance on the first day of the season was calculated as the estimated abundance on the last day of the pre-season survey (day 205), discounted for natural mortality acting over the intervening 3-day period (no fishing occurred during this time):

$$\widehat{N}_{208} = \widehat{N}_{205} e^{-M(208-205)}$$

The abundance on the last day of the pre-season survey was calculated as the survey biomass divided by the average GAM-predicted individual squid weight for the survey:

$$\widehat{N}_{205} = \frac{\hat{B}_{survey}}{\widehat{w}_{survey}}$$

Combining the above equations leads to:

$$\hat{q} = \frac{\frac{CPUE(B)_{208}}{\widehat{w}_{208}}}{\frac{\hat{B}_{survey}}{\widehat{w}_{survey}} e^{-3M}}$$

Variables w_{208}, w_{survey}, B_{survey} and M were assumed normally distributed, parameterised with the mean and standard deviation obtained from the pre-season survey biomass report (B_{survey}), calculated from the individual *D. gahi* weight data during the pre-season survey (w_{208}, w_{survey}), or adapted from the literature (M):

$$B_{survey} \sim \mathcal{N}(14{,}231, 4{,}982^{a})$$

$$w_{208} \sim \mathcal{N}(0.03169, 0.00051)$$

$$w_{survey} \sim \mathcal{N}(0.03163, 0.00059)$$

$$M \sim \mathcal{N}(0.01534, 0.00487)$$

The prior distribution of q was obtained by randomly sampling 100,000 values from the distributions of w_{208}, w_{survey}, B_{survey}, and M, and randomly resampling the observed 16 values of $CPUE(B)_{208}$ 100,000 times with replacement, and recalculating q. The resulting distribution of 100,000 q values was fitted with gamma and lognormal distributions, appropriate for strictly positive continuous data. The lognormal distribution provided a better fit; therefore, the q prior was defined as a lognormal distribution parameterised by the mean and standard deviation in log-space:

$$q \sim \mathcal{LN}(-6.483, 0.492)$$

5.2. Model weighting

Relative weights in the joint optimisation were assigned to the data and the prior as the converse of their coefficients of variation (CV). The CV of the data was calculated as the normalised root mean squared deviation (NRMSD) of the differences between the observed daily catches in numbers and predicted catches from a depletion model fitted without utilising prior information on catchability.

$$CV_{data} = NRMSD = \frac{\sqrt{\frac{1}{T}\sum_t (X_t - C_t)^2}}{\frac{1}{T}\sum_t (X_t)}$$

where X_t and C_t are the observed and predicted catch on day of the season t, and T is the season duration. The CV of the lognormal prior was calculated as:

$$CV_{prior} = \sqrt{e^{\sigma^2} - 1}$$

[a] Current pre-season survey biomass estimate in the south sub-area had a coefficient of variation CV = 0.13. Payá (2010) had estimated average net escapement of up to 22% during pre-season surveys, which was added to the current survey biomass estimate CV (0.13 + 0.22 = 0.35). Revised standard deviation was then calculated as 14,231 t * 0.35 = 4,982 t. The 22% escapement was added as a linear increase in the variability, but was not used to increase the total estimate, because squid that escape one trawl are likely to be part of the biomass concentration that is available to the next trawl.

where σ is the standard deviation in log-space. CV_{data} was calculated separately for the south and north sub-area models. As the prior of q was assumed identical for the north and south sub-areas, CV_{prior} was shared by the two models.

5.3. Model fit

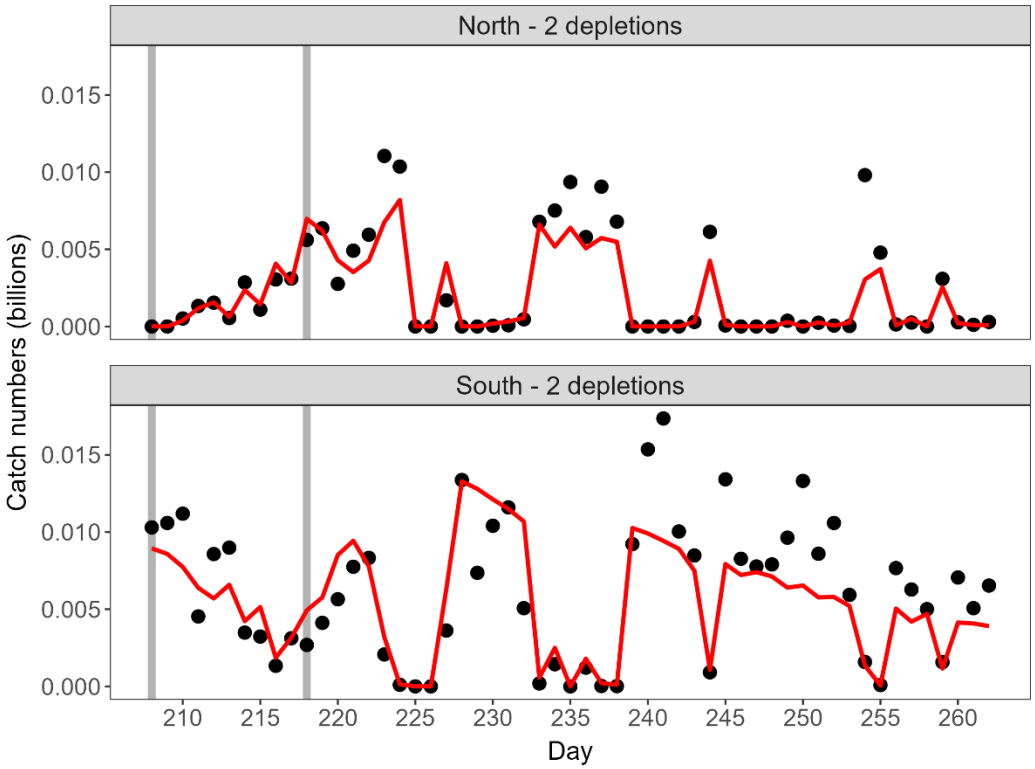

Figure A.1. Model fit (red lines) to the observed catch in numbers (black dots). Grey bars indicate immigration peaks (days 208 and 218).

5.4. Parameter estimates

For the north sub-area, MPD parameter estimates were: $N1_{(\text{day } 208)} = 0.275 \times 10^9$, $N2_{(\text{day } 218)} = 0.196 \times 10^9$, and $q = 1.503 \times 10^{-3}$ vessel-day^{-1}. Posterior distributions of estimated parameters for the north sub-area are given in Figure A.2. Posterior distribution of q was much narrower than its prior distribution, suggesting that the data were informative about q.

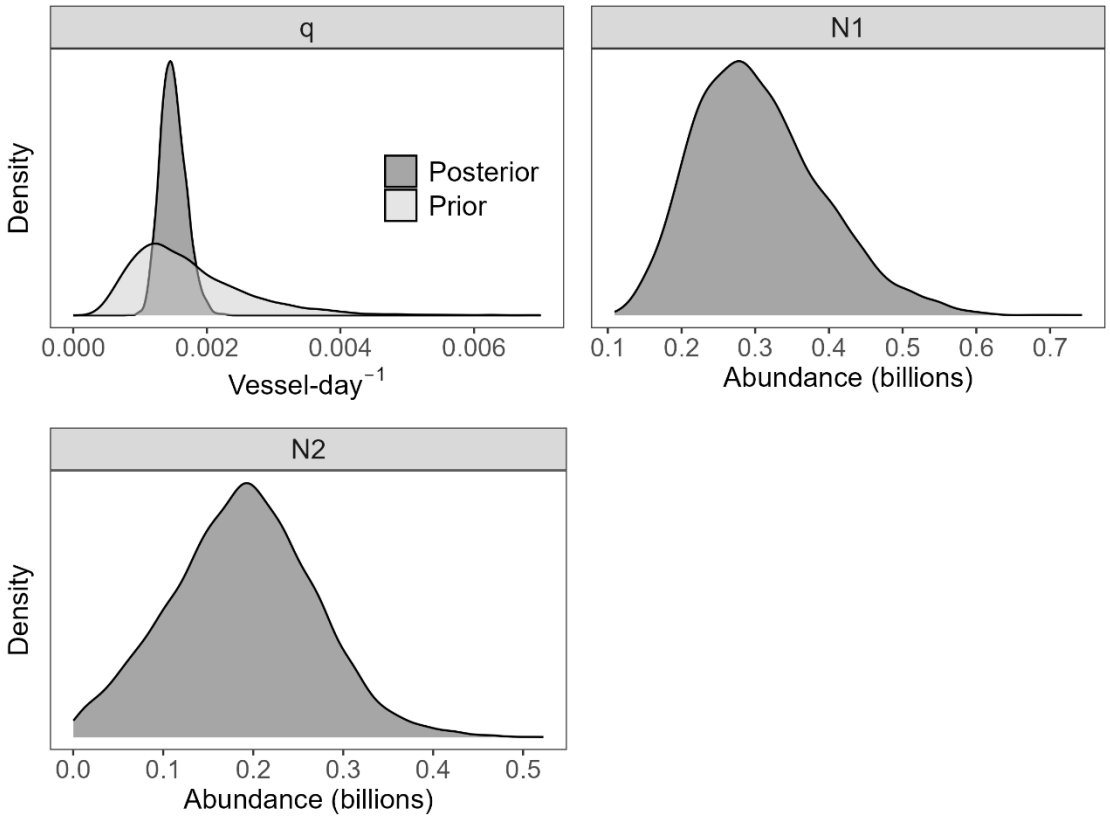

Figure A.2. Prior (light grey) and posterior distributions (dark grey) of estimated parameters for the north sub-area. Note that only catchability q has a prior (the same prior is used for north and south models).

For the south sub-area, MPD parameter estimates were: $N1_{(\text{day } 60)} = 0.414 \times 10^9$, $N2_{(\text{day } 75)} = 0.458 \times 10^9$, and $q = 1.359 \times 10^{-3}$ vessel-day^{-1}. Posterior distributions of estimated parameters are given in Figure A.3. Posterior distribution of q was much narrower than its prior distribution, suggesting that the data were informative about q.

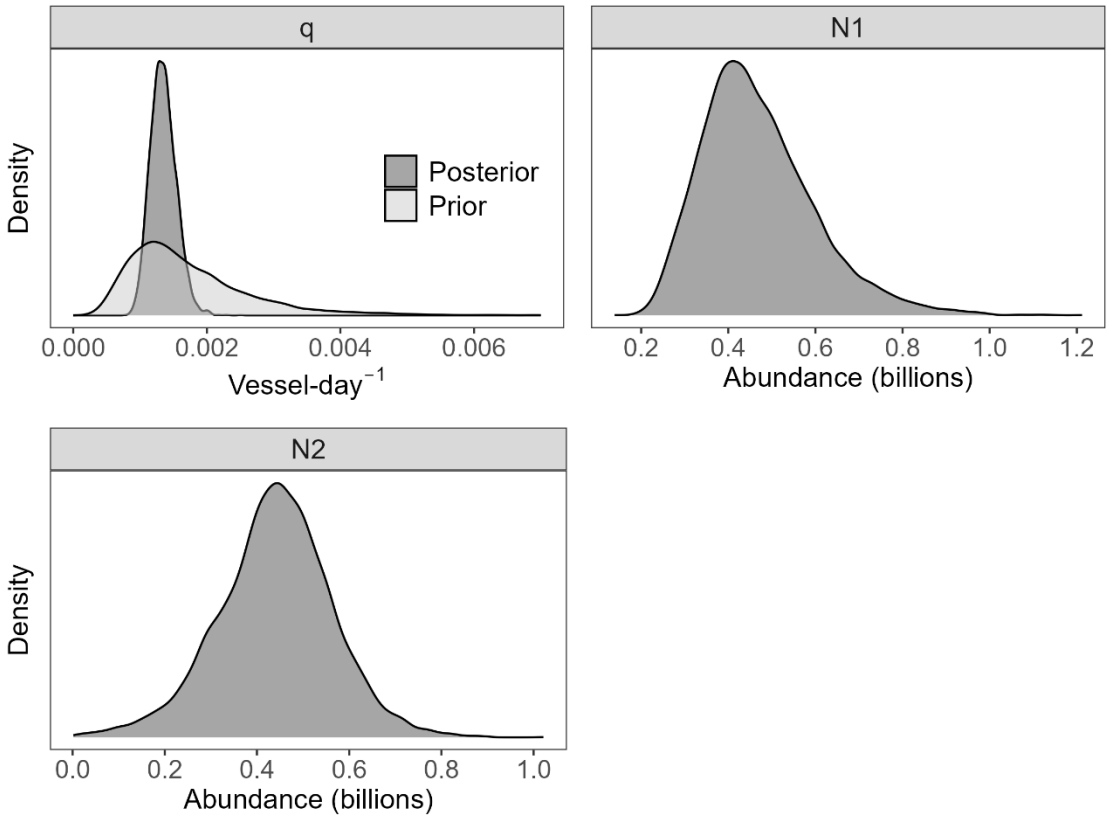

Figure A.3. Prior (light grey) and posterior distributions (dark grey) of estimated parameters for the south sub-area. Note that only catchability q has a prior (the same prior is used for north and south models).

5.5. MCMC diagnostics

North sub-area

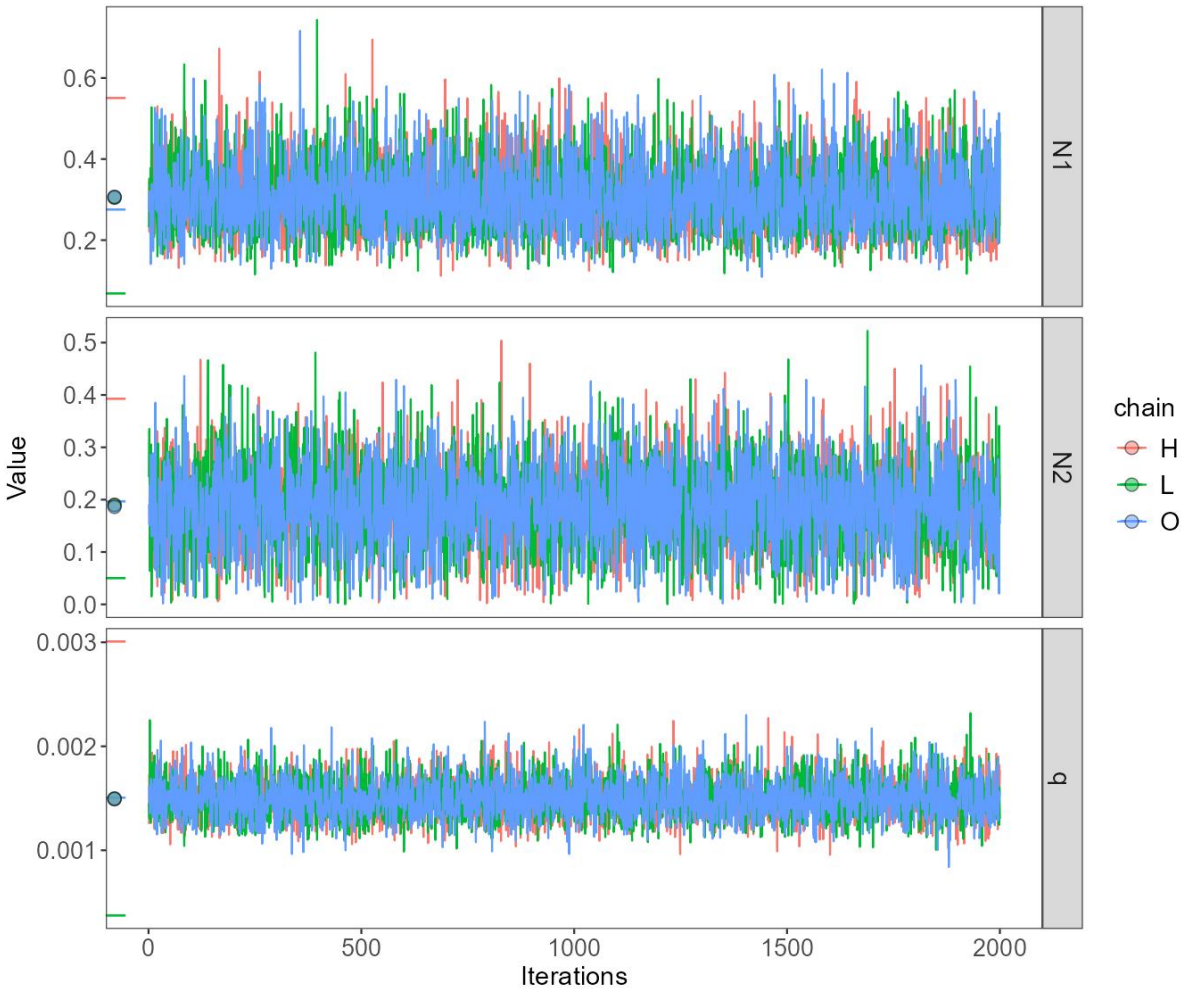

Figure A.4. MCMC posterior trace plots of estimated parameters for the north sub-area, after burn-in and thinning. Colours denote chains initiated at different starting values (H – high, L – low, O – optimal). Horizontal line segments: starting values of the three chains. Dots: mean values of the three chains.

Table A.1. MCMC convergence diagnostic results for the north sub-area: Geweke's single-chain stationarity test and Heidelberger and Welch's stationarity and half-width tests.

Parameter	Chain	Geweke's stationarity test		Heidelberger and Welch's stationarity test		Heidelberger and Welch's halfwidth test		
		p-value	outcome	p-value	outcome	mean	halfwidth	outcome
N1	H	0.209	passed	0.083	passed	0.306	0.004	passed
	L	0.339	passed	0.235	passed	0.305	0.004	passed
	O	0.917	passed	0.812	passed	0.307	0.004	passed
N2	H	0.485	passed	0.32	passed	0.19	0.003	passed
	L	0.355	passed	0.068	passed	0.19	0.004	passed
	O	0.411	passed	0.702	passed	0.186	0.004	passed
q	H	0.395	passed	0.549	passed	0.001	0	passed
	L	0.897	passed	0.702	passed	0.001	0	passed
	O	0.848	passed	0.696	passed	0.001	0	passed

Table A.2. MCMC convergence diagnostic results for the north sub-area: Gelman and Rubin's convergence diagnostic for parallel chains.

Parameter	Gelman-Rubin convergence diagnostic ($\hat{R}$)	Convergence ($\hat{R} < 1.1$)	Multivariate version $\hat{R}$	Convergence ($\hat{R} < 1.1$)
N1	1.00123	passed		
N2	1.000991	passed	1.000573	passed
q	0.999653	passed		

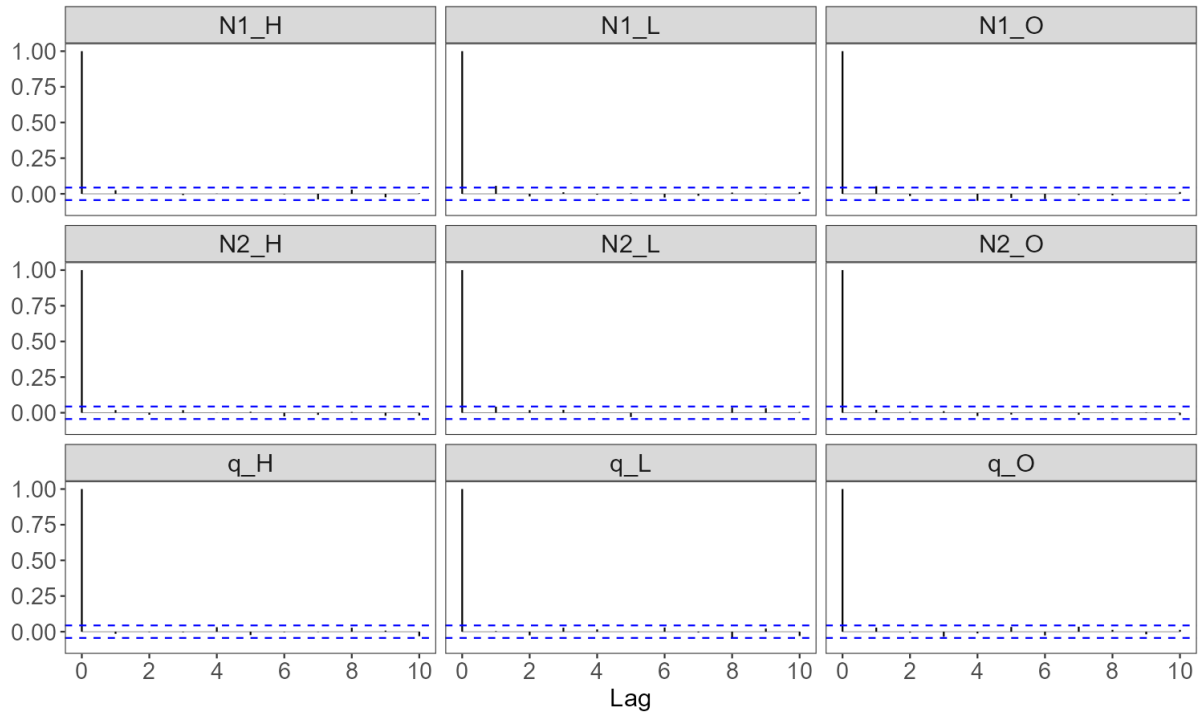

Figure A.5. MCMC autocorrelation lag plots of the estimated parameters for the north sub-area.

South sub-area

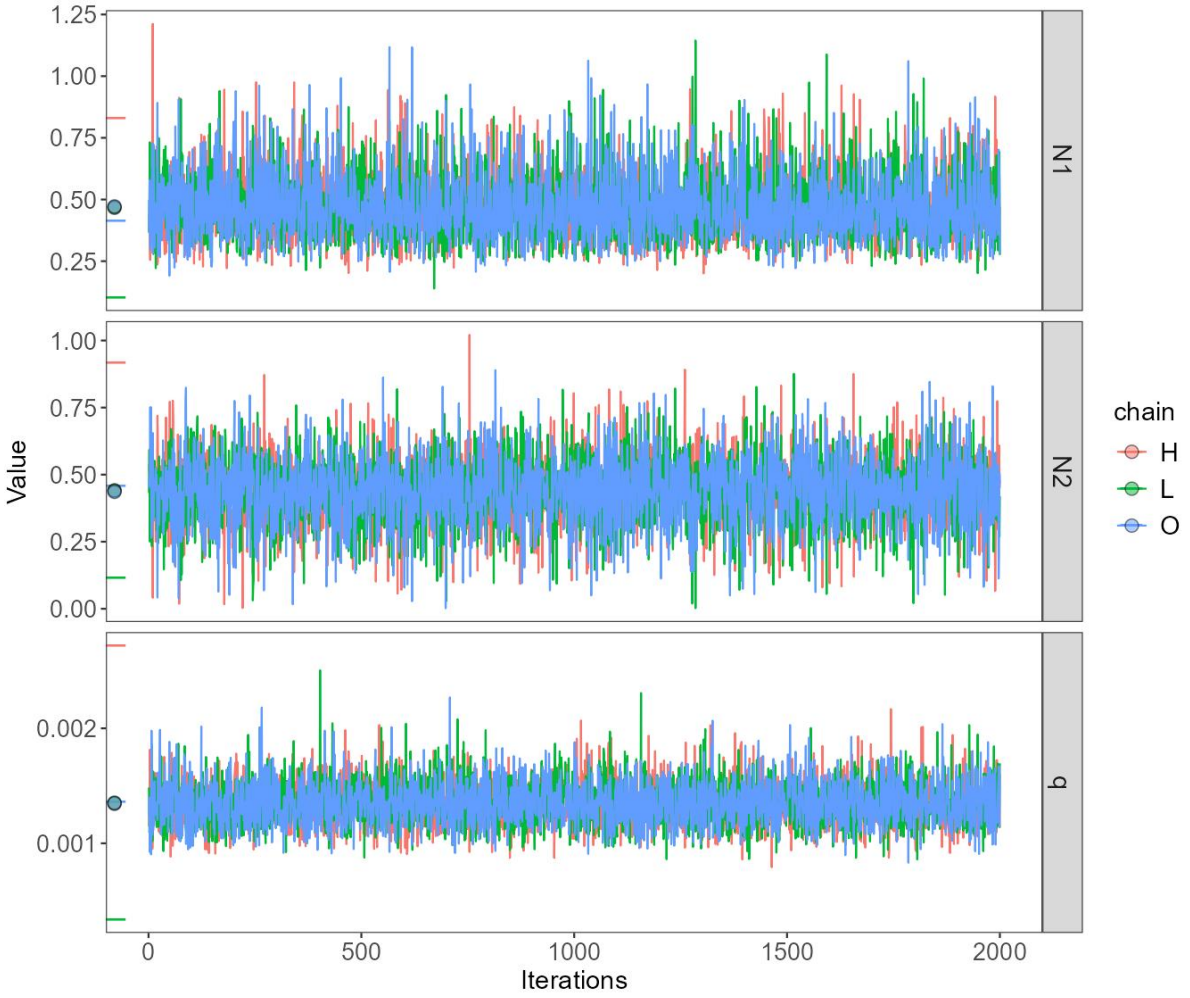

Figure A.6. MCMC posterior trace plots of estimated parameters for the south sub-area, after burn-in and thinning. Colours denote chains initiated at different starting values (H – high, L – low, O – optimal). Horizontal line segments: starting values of the three chains. Dots: mean values of the three chains.

Table A.1. MCMC convergence diagnostic results for the south sub-area: Geweke's single-chain stationarity test and Heidelberger and Welch's stationarity and half-width tests.

Parameter	Chain	Geweke's stationarity test		Heidelberger and Welch's stationarity test		Heidelberger and Welch's halfwidth test		
		p-value	outcome	p-value	outcome	mean	halfwidth	outcome
N1	H	0.324	passed	0.246	passed	0.469	0.006	passed
	L	0.112	passed	0.479	passed	0.466	0.006	passed
	O	0.45	passed	0.088	passed	0.472	0.006	passed
N2	H	0.101	passed	0.093	passed	0.441	0.005	passed
	L	0.572	passed	0.741	passed	0.441	0.006	passed
	O	0.475	passed	0.158	passed	0.436	0.006	passed
q	H	0.063	passed	0.674	passed	0.001	0	passed
	L	0.15	passed	0.308	passed	0.001	0	passed
	O	0.694	passed	0.277	passed	0.001	0	passed

Table A.2. MCMC convergence diagnostic results for the south sub-area: Gelman and Rubin's convergence diagnostic for parallel chains.

Parameter	Gelman-Rubin convergence diagnostic ($\hat{R}$)	Convergence ($\hat{R} < 1.1$)	Multivariate version $\hat{R}$	Convergence ($\hat{R} < 1.1$)
N1	1.000269	passed		
N2	1.000212	passed	1.000021	passed
q	1.000418	passed		

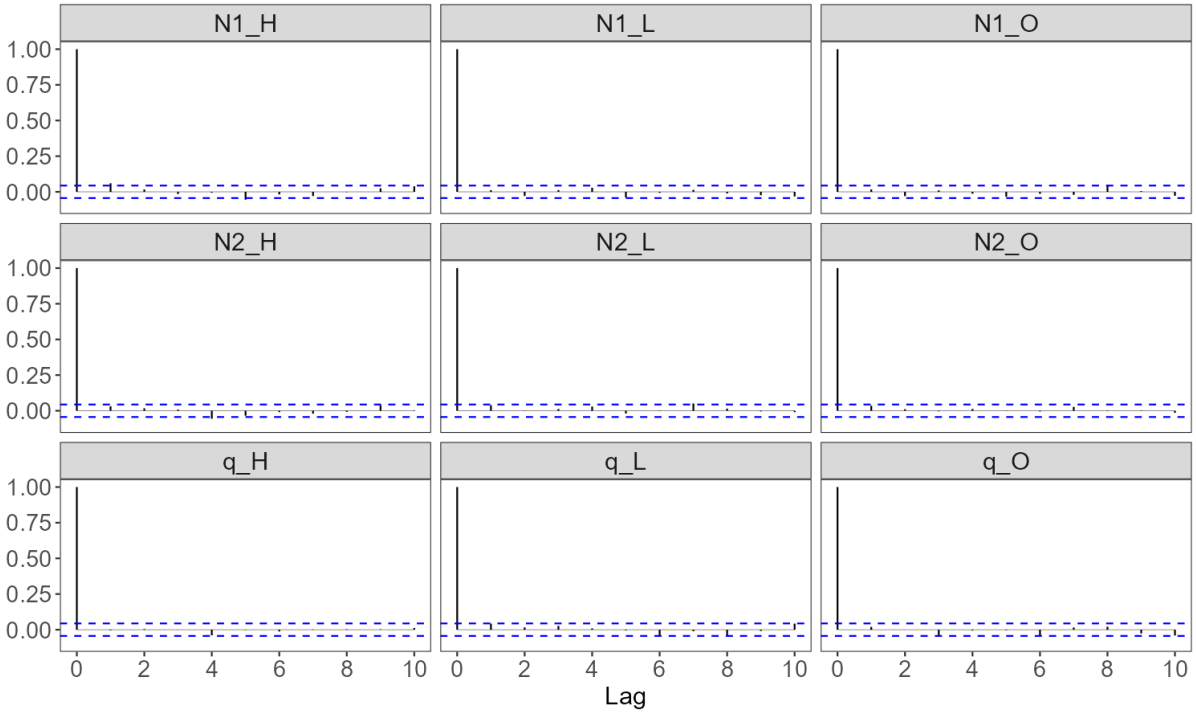

Figure A.7. MCMC autocorrelation lag plots of the estimated parameters for the south sub-area.

5.6. Catch composition

Table A.5. Total reported catch and discard by taxon during the 2nd season 2025 X-license fishing, and percentage of vessel-days in which each taxon occurred. Does not include incidental catches of pinnipeds or seabirds.

Species Code	Species / Taxon	Catch (kg)	Discard (kg)	Occurrence (%)
LOL	*Doryteuthis gahi*	18,454,068	38,907	100.0
HAK	*Merluccius hubbsi*	716,135	14,180	91.6
PAR	*Patagonotothen ramsayi*	370,213	370,181	95.3
ZYP	*Zygochlamys patagonica*	101,095	99,745	83.3
MED	Scyphozoa	28,544	28,544	54.0
PTE	*Patagonotothen tessellata*	27,528	27,521	41.7
CGO	*Cottoperca gobio*	22,181	22,124	85.7
OTH	Actinopterygii	13,213	13,213	21.5
AST	Asteroidea	10,857	10,857	18.1
RAY	Rajiformes	10,849	9,472	79.6
TOO	*Dissostichus eleginoides*	7,629	7,628	54.8
DGH	*Schroederichthys bivius*	6,975	6,975	66.2
BAC	*Salilota australis*	6,056	430	12.3
LIM	*Lithodes murrayi*	5,443	5,421	21.5
CRB	*Lithodes* sp.	4,496	4,496	16.0
UCH	*Strongylocentotus* spp.	3,796	3,796	14.1
SPN	Spongiidae	2,462	2,462	12.2
OCT	*Eledone* spp.	1,766	1,766	27.2
ILL	*Illex argentinus*	1,597	769	26.4
LIT	*Lithodes turkayi*	1,527	1,527	11.8
ING	*Moroteuthopsis ingens*	1,427	1,427	28.1
MYX	Myxinidae	1,226	1,207	25.1
MUN	*Grimothea gregaria*	624	624	4.0
DGS	*Squalus acanthias*	612	612	11.5
NED	*Neolithodes diomedeae*	594	594	4.0
GRV	*Macrourus* spp.	279	279	5.8
MUL	*Eleginops maclovinus*	235	232	6.1
EEL	*Iluocoetes fimbriatus*	189	189	7.0
KIN	*Genypterus blacodes*	122	122	3.1
WHI	*Macruronus magellanicus*	64	64	4.5
PAT	*Merluccius australis*	62	62	1.5
BLU	*Micromesistius australis*	40	40	2.7
RED	*Sebastes oculatus*	33	33	1.4
COP	*Congiopodus peruvianus*	32	32	0.5
CHE	*Champsocephalus esox*	26	26	2.4
ALF	*Allothunnus fallai*	22	22	0.5
NEM	*Psychrolutes marmoratus*	22	22	1.5
SAR	*Sprattus fuegensis*	22	22	0.9
BDU	*Brama australis*	14	14	0.8

SEP	*Seriolella porosa*	13	13	0.5
LAR	*Lampris immaculatus*	8	8	0.1
BUT	*Stromateus brasiliensis*	5	5	0.4
MAR	*Martialia hyadesi*	2	2	0.4
NOW	*Paranotothenia magellanica*	1	1	0.1
COX	*Patagonotothen* spp.	0	0	0.1
GRF	*Coelorinchus fasciatus*	0	0	0.1
MAM	*Neoachiropsetta milfordi*	0	0	0.1
ROK	*Helicolenus* spp.	0	0	0.1
Total		19,802,104	675,666	